documented in and around the area of hepatocyte damage [13, 14].

Tropomyosin is one of the actin-associated proteins, present in virtually all eukaryotic cells, and modulates the interaction between actin and myosin to stabilize the actin-filament structure. Tropomyosin assembles into an α-helical coiled heterodimer composed of an α-chain and a β-chain, with each molecule interacting with six or seven monomers of actin [15, 16]. Tropomyosin regulates the contractility of striated muscle by blocking myosin-binding sites on actin in the relaxed state. On activation, tropomyosin moves away from these sites [17]. X-ray studies have suggested that the initiation of smooth muscle contraction leads to the movement of tropomyosin in a manner similar to that in striated muscle [18]. Although one recent study has shown the expression and organization of actin filaments and tropomyosin in the cloned hepatic GRX cell line [19], tropomyosin expression patterns in primary cultured HSCs and the fibrotic liver remain to be studied.

This study aimed to demonstrate the presence of tropomyosin in HSCs and clarify the dynamics of its expression pattern during HSC activation. Herein, we report in detail the expression pattern of tropomyosin in cultured rat HSCs and fibrotic liver tissue induced in rats by thioacetamide (TAA) administration, and further demonstrate the network of α-SMA filaments and tropomyosin in primary HSC cultures.

Materials and methods

Materials

Collagenase was purchased from Wako Pure Chemical Co. (Osaka, Japan). Pronase E was obtained from Merck (Damstadt, Germany). Mouse monoclonal IgG2a antibody against α-SMA, mouse monoclonal IgG1 antibody against tropomyosin, Dulbecco's modified Eagle's medium (DMEM), TAA, and fetal bovine serum (FBS) were purchased from Sigma Chemical Co. (Saint Louis, MO, USA). Rabbit polyclonal IgG antibodies against human platelet-derived growth factor receptor-β (PDGFR-β) that reacts with rat PDGFR-β were purchased from Santa Cruz Biotechnology (Santa Cruz, CA, USA). Horseradish peroxidase-conjugated secondary antibodies against mouse and rabbit immunoglobulins were obtained from Dako. Alexa Fluor 488 goat antimouse IgG2a antibodies and Alexa Fluor 594 goat antimouse IgG1 antibodies were from Molecular Probes (Eugene, OR, USA). ECL immunoblotting detection reagent was purchased from Amersham Pharmacia Biotech (Buckinghamshire, England). Immobilon P membranes were from Millipore Corp. (Bedford, MA, USA). Cell culture inserts were from Falcon (Beckton Dickinson, Franklin Lakes, NJ, USA). All the other reagents were purchased from Sigma Chemical Co. or Wako Pure Chemical Co.

Animals

Pathogen-free male Wistar rats (12-week-old, body weight 200–220 g) were obtained from SLC (Shizuoka, Japan). Animals were housed at a constant temperature and supplied with laboratory chow and water ad libitum. The protocol of the experiments was approved by the Animal Research Committee of Osaka City University (Guide for Animal Experiments, Osaka City University).

Induction of liver fibrosis

Liver fibrosis was induced in rats ($n = 3$) by the intraperitoneal injection of TAA (40 mg/body weight) dissolved in 2 ml of saline twice a week for up to 10 weeks. Control rats ($n = 3$) were given 2 ml of saline during the same period.

Preparation of HSCs

HSCs were isolated from male Wistar rats, as previously described in detail [20]. Isolated HSCs were suspended in DMEM supplemented with 10% FBS at a cell density of 5×10^5 cells/ml, and 1.5 ml of the cell suspension was introduced into a 35-mm cell tissue culture plate (Falon, 3003). After the culture had continued for the indicated number of days, the cells were fixed in 4% paraformaldehyde solution for immunocytochemistry or lysed for immunoblotting.

Immunoblotting

Protein samples (10 μg) were subjected to SDS-PAGE and then transferred onto Immobilon P membranes. After blocking, the membranes were treated with primary antibodies and then with peroxidase-conjugated secondary antibodies. Immunoreactive bands were visualized using the ECL system (Amersham Pharmacia Biotech) and documented by LAS 1000 (Fuji Photo Film, Kanagawa, Japan). The density of bands was analyzed using a BIO-RAD GS-700 densitometer. Experiments were repeated thrice using samples obtained from HSCs isolated from different rats.

Immunohistochemistry and collagen staining

Immunohistochemistry was performed using the methods described in detail elsewhere [21]. After the development of fibrosis, rats were anesthetized and laparotomized. The

liver was perfused with phosphate-buffered saline (PBS) and then perfusion-fixed with 4% formaldehyde, dehydrated, and embedded in Polybed. Sections were cut at a thickness of 5 μm and stained for 1 h in 0.1% (w/v) Sirius red (Direct Red 80, Aldrich, Milwaukee, WI, USA) [22]. Double immunostaining analysis was carried out using methods described previously [22]. After blocking with 5% bovine serum albumin/PBS, they were incubated overnight with primary antibodies in the medium. They were then incubated with both 20 μg/ml Alexa Fluor 488 goat anti-mouse IgG2a antibody and 20 μg/ml Alexa Fluor 594 goat anti-mouse IgG1 antibody for 2 h. Specimens were counterstained for nuclei with DAPI. The sections were observed under an LSM510 confocal laser scanning microscope (Carl Zeiss, Germany).

Cultured HSCs on glass microscope slides were fixed with 3.7% formaldehyde for 30 min at room temperature. After washing thrice with PBS containing 0.1% Triton X-100, the fixed cells were incubated with anti-α-SMA antibody and anti-tropomyosin antibody for 1 h at room temperature and successively with FITC-labeled goat antimouse IgG1 (Alexa Fluor 488) and rhodamine-labeled goat antimouse IgG2a (Alexa Fluor 594) for 1 h at room temperature. After washing, the specimens were observed under an LSM510 confocal laser scanning microscope (Carl Zeiss, Germany). Experiments were repeated thrice using samples obtained from HSCs isolated from different rats.

Immunohistochemical analysis of human liver samples

One specimen obtained by resection during surgery from subjects with normal liver function was used as a control. Informed written consent was obtained from all patients at the time of their liver biopsy, and the study was conducted in conformance with the Helsinki Declaration. The diagnosis of liver cirrhosis was established on the basis of the clinical and histopathological features. Immunohistochemistry was performed according to the methods described above.

Results

Tropomyosin expression in primary cultured HSCs

We investigated the expression of tropomyosin in primary-cultured HSCs as a model because HSC culture precisely resembles the in vivo cellular phenotypic change of HSCs from a vitamin A-storing quiescent phenotype to an activated and myofibroblastic phenotype in response to inflammatory stimuli [23]. Freshly isolated and plated HSCs resembled lipocytes, extended branching cytoplasmic processes, and enclosed multiple droplets that contained retinol (Fig. 1Aa). After culturing for 3 days, the cells expanded their cell body with enlarged processes and nuclei, and the size of fat droplets decreased (Fig. 1Ab). By

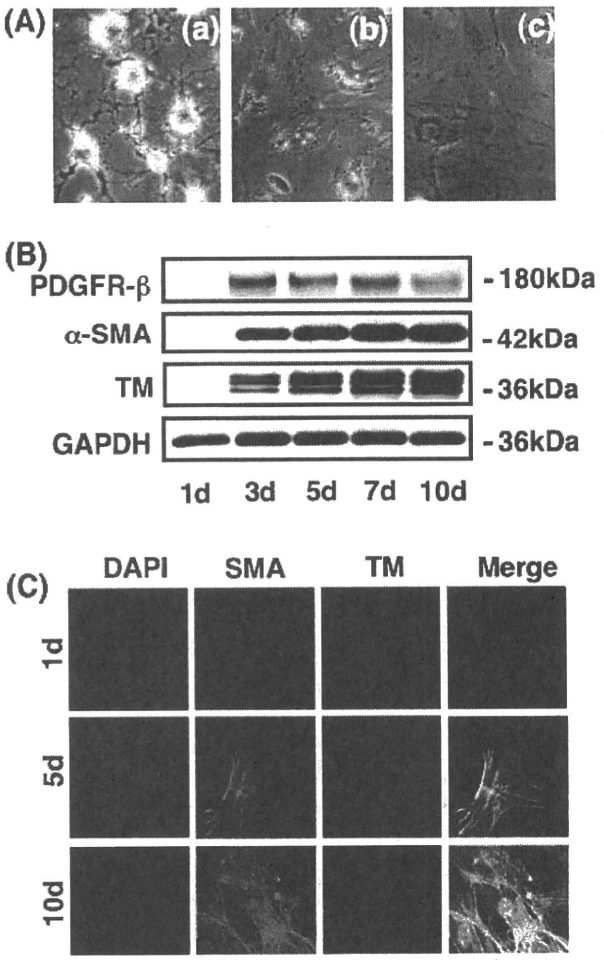

Fig. 1 Tropomyosin expression in primary cultured HSCs. **A** The cell morphology of isolated and cultured HSCs was observed under phase-contrast microscopy everyday, monitored, and digitally recorded. **a** Day 1. HSCs attached to the plate enclose droplets that contain vitamin A. **b** Day 3. HSCs start extending their processes. **c** Day 7. HSCs showed enlarged cell body and lose their droplets (magnification, ×200). **B** The expression of tropomyosin in cultured HSCs was determined by immunoblot and immunocytochemistry. Whole-cell homogenates were subjected to SDS-PAGE, transferred onto the membrane, and successively immunoreacted with PDGFR-β, α-SMA, or tropomyosin. Note that tropomyosin is induced in HSCs time dependently after starting the culture in a manner similar to the expression of PDGFR-β and α-SMA. Representative data from three independent preparations are presented here. **C** Immunocytochemistry of tropomyosin and α-SMA. Cultured HSCs on days 1, 5, and 10 were fixed in 4% paraformaldehyde and subjected to immunocytochemistry, as described in section "Materials and methods". Note that tropomyosin appears on day 5 and becomes prominent on day 10. Tropomyosin colocalizes and generates stress fibers with α-SMA (magnification ×200)

day 7, most of the cells had lost their fat droplets, spread more prominently, and appeared "myofibroblastic" (Fig. 1Ac). These observations are in good agreement with previous reports [1, 6, 21].

As shown in Fig. 1B, immunoblot analysis showed that bands for tropomyosin at molecular weights of 36–39 kDa [24] were invisible in freshly isolated HSCs, started to appear in them after being cultured for 3 days, and thereafter increased in a time-dependent manner. The relative level of tropomyosin evaluated by densitometric normalization against GAPDH gradually increased with culture prolongation (data not shown). The multiple bands detected are considered to be related to post-transcriptional modification, particularly N-terminal acetylation, of the protein, as described elsewhere [25]. Tropomyosin induction took place in a similar manner to that of α-SMA and PDGFR-β (Fig. 1B). These observations were further confirmed by immunocytochemistry. α-SMA became readily detectable on day 1 and was uniformly distributed in the cytoplasm. HSCs cultured for more than 5 days exhibited a flattened and stretched morphology with developed stress fibers, which consisted of α-SMA (Fig. 1C). Tropomyosin was negligible on day 1, but was visible and co-localized with α-SMA at day 5, and then exhibited prominent stress fibers crossing the cytoplasm together with α-SMA bundles (Fig. 1C).

Expression of tropomyosin in fibrotic livers

Tropomyosin induction in culture-activated HSCs prompted us to investigate its expression in liver tissue. As shown in Fig. 2A, total protein extracted from rat livers treated with TAA for 6 or 10 weeks cross-hybridized to α-SMA and tropomyosin antibodies, whereas virtually no hybridization was observed in the total extraction from an intact rat liver. This result indicates that tropomyosin is not ubiquitously expressed in liver-constituent cells such as hepatocytes, Kupffer cells, and endothelial cells. The level of tropomyosin in the liver homogenate increased in a time-dependent manner after TAA administration, similar to the induction of PDGFR-β and α-SMA. Collagen deposition was prominent in the liver after a 10-week TAA administration, as shown on Sirius red staining. Tropomyosin was found to be present along the fibrotic septum, although it was rarely seen in the intact liver (Fig. 2B). Double immunostaining of α-SMA and tropomyosin confirmed that these two proteins co-existed in and around the fibrotic septum and were hardly present in "pseudolobular" parenchyma where no fibrosis was obvious (Fig. 2C). However, activated HSCs that were present close to the septum and positive for α-SMA also expressed tropomyosin (Fig. 2C, high), indicating both activated HSCs and septum-forming myofibroblasts ubiquitously expressed

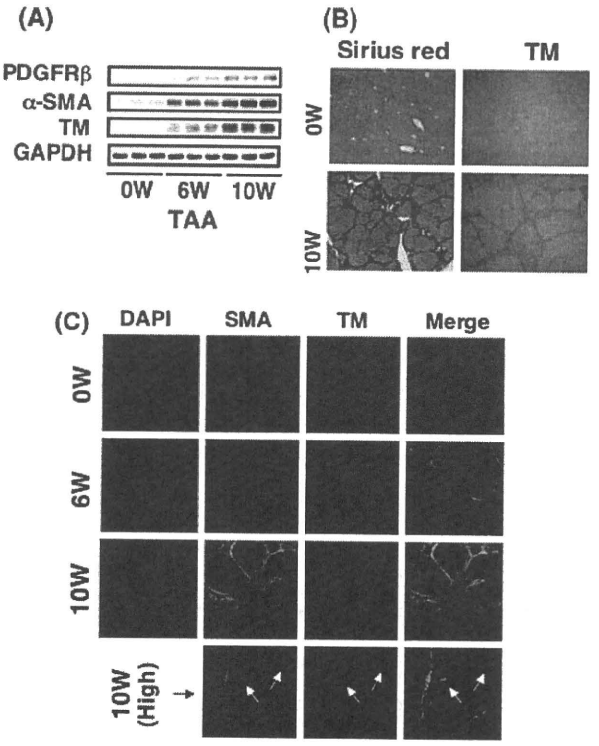

Fig. 2 Expression of tropomyosin in fibrotic livers. The expression of tropomyosin in the fibrotic liver was determined by immunoblot and immunohistochemistry. **A** Whole-liver homogenates were subjected to SDS-PAGE, transferred onto the membrane, and successively immunoreacted with PDGFR-β, α-SMA, or tropomyosin. Note that tropomyosin is induced in the liver of rats treated with TAA time dependently after starting injection in a similar manner to the expression of PDGFR-β and α-SMA. **B** Histology. Prominent liver fibrosis is observed in the liver of rats treated with TAA for 10 weeks by Sirius red staining. Tropomyosin expression is clear along the septa. **C** Fluorescent immunohistochemistry of tropomyosin and α-SMA. Double immunostaining was performed in the liver of rats treated with TAA for 6 and 10 weeks. Note that both proteins always colocalize and are expressed strongly at the site between noninjurious parenchyma and septa (magnification ×100). Activated HSCs (*arrows*) that were present close to the septum and positive for α-SMA also expressed tropomyosin (magnification ×400)

tropomyosin. A strong linear-pattern expression of these proteins at the site between the septum and the parenchyma was notable. Tropomyosin expression was rarely observed in intact human liver, while it was localized along the fibrotic septum in human cirrhosis (Fig. 3).

Discussion

Activated HSCs express α-SMA as contractile machinery. Although accumulated studies have evaluated the importance of α-SMA and other cytoskeletons filaments on HSC contraction, there has been no report on the expression of tropomyosin, which is one of the components of actin

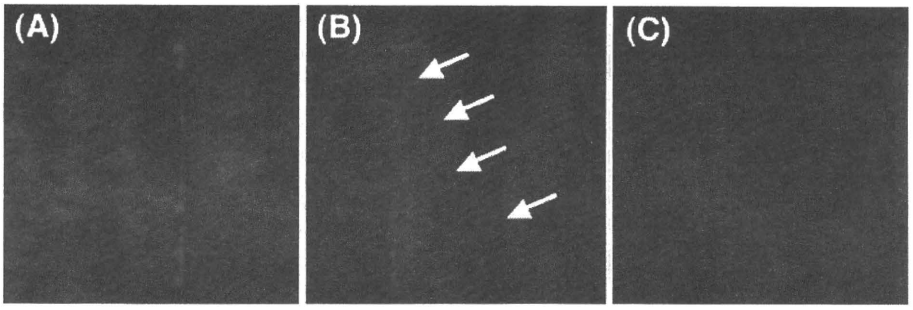

Fig. 3 Expression of tropomyosin in human livers. The expression of tropomyosin in the human liver was determined by immunohistochemistry. **A** Intact human liver. **B** Cirrhosis caused by hepatitis C infection. **C** Negative control stained without antitropomyosin antibody (magnification ×200)

filaments and calcium-binding proteins and plays a major role in the contraction process of smooth muscle, in HSCs and fibrotic liver tissue. The key molecular function of tropomyosin is to shield and unshield the binding site of myosin to actin [15, 16]. Thus, tropomyosin is speculated to play a pivotal role also in the contraction of HSCs. In the present study, we report for the first time that the expression of tropomyosin is found predominantly in activated HSCs and to be as high as α-SMA. These observations suggest that tropomyosin is a regulatory protein which counteracts or triggers the contraction of HSCs due to its calcium-binding status. In fact, HSC contraction is reportedly induced by endothelin-1, angiotensin II, and thrombin, which are all intracellular calcium inducers [23].

HSCs are considered to be more contractile at presinusoidal terminal portal venules in the injured liver, as indicated by the high-level expression of endothelin-1 receptors [26]. HSCs localized at this site also generate endothelin-1 and angiotensin-II, that are responsible molecules for portal hypertension, a pathological process induced by constriction of the hepatic vasculature [27, 28]. As a consequence, tropomyosin expressed at the site between the septum and the parenchyma is speculated to play a positive regulatory role in actin–myosin association and contribute to presinusoidal portal rigidity.

In conclusion, the present findings indicate that tropomyosin could be a novel marker for activated HSCs in vivo as well as in culture and be utilizable for a clinical diagnosis of liver fibrosis.

Acknowledgment This work was supported by the Grants-in-Aid from the Japan Society for the Promotion of Science to NK.

References

1. Blomhoff R, Wake K. Perisinusoidal stellate cells of the liver: important roles in retinol metabolism and fibrosis. FASEB J 1991;5:271–277
2. Friedman SL. Seminars in medicine of the Beth Israel Hospital, Boston. The cellular basis of hepatic fibrosis. Mechanisms and treatment strategies. N Engl J Med 1993;328:1828–1835. doi:10.1056/NEJM199306243282508
3. Okuyama H, Shimahara Y, Kawada N. The hepatic stellate cell in the post-genomic era. Histol Histopathol 2002;17:487–495
4. Bataller R, Brenner DA. Hepatic stellate cells as a target for the treatment of liver fibrosis. Semin Liver Dis 2001;21:437–451. doi:10.1055/s-2001-17558
5. Ramadori G, Veit T, Schwögler S, Dienes HP, Knittel T, Rieder H, et al. Expression of the gene of the alpha-smooth muscle-actin isoform in rat liver and in rat fat-storing (ITO) cells. Virchows Arch 1990;59:349–357
6. Kawada N, Klein H, Decker K. Eicosanoid-mediated contractility of hepatic stellate cells. Biochem J 1992;285:367–371
7. Rockey DC, Boyles JK, Gabbiani G, Friedman SL. Rat hepatic lipocytes express smooth muscle actin upon activation in vivo and in culture. J Submicrosc Cytol Pathol 1992;24:193–203
8. Rockey DC, Housset CN, Friedman SL. Activation-dependent contractility of rat hepatic lipocytes in culture and in vivo. J Clin Invest 1993;92:1795–1804. doi:10.1172/JCI116769
9. Kawada N, Tran-Thi TA, Klein H, Decker K. The contraction of hepatic stellate (Ito) cells stimulated with vasoactive substances. Possible involvement of endothelin 1 and nitric oxide in the regulation of the sinusoidal tonus. Eur J Biochem 1993;213:815–823. doi:10.1111/j.1432-1033.1993.tb17824.x
10. Skalli O, Ropraz P, Trzeciak A, Benzonana G, Gillessen D, Gabbiani G. A monoclonal antibody against alpha-smooth muscle actin: a new probe for smooth muscle differentiation. J Cell Biol 1986;103:2787–2796. doi:10.1083/jcb.103.6.2787
11. Bhunchet E, Wake K. Role of mesenchymal cell populations in porcine serum-induced rat liver fibrosis. Hepatology 1992;16:452–1473. doi:10.1002/hep.1840160623
12. Rockey DC, Chung JJ. Endothelin antagonism in experimental hepatic fibrosis. Implications for endothelin in the pathogenesis of wound healing. J Clin Invest 1996;98:1381–1388. doi:10.1172/JCI118925
13. Sakaida I, Nagatomi A, Hironaka K, Uchida K, Okita K. Quantitative analysis of liver fibrosis and stellate cell changes in patients with chronic hepatitis C after interferon therapy. Am J Gastroenterol 1999;94:489–496. doi:10.1111/j.1572-0241.1999.884_m.x
14. Martinelli AL, Ramalho LN, Zucoloto S. Hepatic stellate cells in hepatitis C patients: relationship with liver iron deposits and severity of liver disease. J Gastroenterol Hepatol 2004;19:91–98. doi:10.1111/j.1440-1746.2004.03255.x
15. Hitchcock-DeGregori SE, Varnell TA. Tropomyosin has discrete actin-binding sites with sevenfold and fourteenfold periodicities. J Mol Biol 1990;214:885–896. doi:10.1016/0022-2836(90)90343-K
16. McLachlan AD, Stewart M. The troponin binding region of tropomyosin. Evidence for a site near residues 197 to 127. J Mol Biol 1976;106:1017–1022. doi:10.1016/0022-2836(76)90349-1
17. Lehrer SS. The regulatory switch of the muscle thin filament: Ca21 or myosin heads? J Muscle Res Cell Motil 1994;15:232–236. doi:10.1007/BF00123476

18. Vibert PJ, Haselgrove JC, Lowy J, Poulsen FR. Structural changes in actin-containing filaments of muscle. J Mol Biol 1972;71:757–767. doi:10.1016/S0022-2836(72)80036-6
19. Mermelstein CS, Guma FC, Mello TG, Fortuna VA, Guaragna RM, Costa ML, et al. Induction of the lipocyte phenotype in murine hepatic stellate cells: reorganisation of the actin cytoskeleton. Cell Tissue Res 2001;306:75–83. doi:10.1007/s004410100428
20. Kristensen DB, Kawada N, Imamura K, Miyamoto Y, Tateno C, Seki S, et al. Proteome analysis of rat hepatic stellate cells. Hepatology 2000;32:268–277. doi:10.1053/jhep.2000.9322
21. Nakatani K, Okuyama H, Shimahara Y, Saeki S, Kim DH, Nakajima Y, et al. Cytoglobin/STAP, its unique localization in splanchnic fibroblast-like cells and function in organ fibrogenesis. Lab Invest 2004;84:91–101. doi:10.1038/sj.labinvest.3700013
22. Nakatani K, Seki S, Kawada N, Kitada T, Yamada T, Sakaguchi H, et al. Expression of SPARC by activated hepatic stellate cells and its correlation with the stages of fibrogenesis in human chronic hepatitis. Virchows Arch 2002;441:466–474. doi:10.1007/s00428-002-0631-z
23. Kawada N. The hepatic perisinusoidal stellate cell. Histol Histopathol 1997;12:1069–1080
24. Somara S, Bitar KN. Tropomyosin interacts with phosphorylated HSP27 in agonist-induced contraction of smooth muscle. Am J Physiol Cell Physiol 2004;286:C1290–C1301. doi:10.1152/ajpcell.00458.2003
25. Gondo K, Ueno T, Sakamoto M, Sakisaka S, Sata M, Tanikawa K. The endothelin-1 binding site in rat liver tissue: light- and electron-microscopic autoradiographic studies. Gastroenterology 1993;104:1745–1749
26. Rockey DC, Weisiger RA. Endothelin induced contractility of stellate cells from normal and cirrhotic rat liver: implications for regulation of portal pressure and resistance. Hepatology 1996;24:233–240. doi:10.1002/hep.510240137
27. Pinzani M, Milani S, De Franco R, Grappone C, Caligiuri A, Gentilini A, et al. Endothelin 1 is overexpressed in human cirrhotic liver and exerts multiple effects on activated hepatic stellate cells. Gastroenterology 1996;110:534–548. doi:10.1053/gast.1996.v110.pm8566602
28. Bataller R, Sancho-Bru P, Gines P, Brenner DA. Liver fibrogenesis: a new role for the renin-angiotensin system. Antioxid Redox Signal 2005;7:1346–1355. doi:10.1089/ars.2005.7.1346

Hepatol Int (2009) 3:497–503
DOI 10.1007/s12072-009-9129-y

ORIGINAL ARTICLE

Effect of natural interferon α on proliferation and apoptosis of hepatic stellate cells

Tomohiro Ogawa · Norifumi Kawada · Kazuo Ikeda

Received: 30 July 2008 / Accepted: 1 April 2009 / Published online: 21 April 2009

Abstract Inhibition of the proliferation of hepatic stellate cells (HSC) is clinically important for the control of liver fibrosis and cirrhosis. Interferons are now frequently used for chronic viral hepatitis because of their anti-viral activity. However, patients treated with interferons exhibit a regression of liver fibrosis even if viral eradication is not achieved, indicating that interferon itself has anti-fibrotic activity. Herein, we show the anti-proliferation and pro-apoptotic activity of natural interferon α against HSC. We found that interferon α inhibited serum-stimulated [^{3}H]thymidine incorporation of HSC in a dose-dependent manner, with a significant reduction at more than 100 U/ml. Interferon α also attenuated PDGF-BB-stimulated DNA synthesis of HSC. Although the molecular mechanism behind these phenomena has not been defined, we found that interferon α triggers the apoptosis of HSC treated with low-dose tumor necrosis factor α, as determined by the Alamar blue assay, morphology, and DNA ladder formation. Furthermore, interferon α decreased inhibitor of caspase-activated DNase (ICAD) levels, which may augment tumor necrosis factor α-induced cell death signals. Thus, interferon α regulates the number of myofibroblastic hepatic stellate cells and may clinically contribute to the regression of human liver fibrosis.

T. Ogawa · N. Kawada (✉)
Department of Hepatology, Graduate School of Medicine, Osaka City University, 1-4-3, Asahimachi, Abeno, 545-8585 Osaka, Japan
e-mail: kawadanori@med.osaka-cu.ac.jp

K. Ikeda
Department of Anatomy, Graduate School of Medicine, Osaka City University, Osaka, Japan

Keywords Tumor necrosis factor α · Caspase · Cyclin · Cytochrome c · Caspase-activated DNase

Introduction

Hepatic stellate cells (HSC), which reside in Disse's space outside sinusoids, maintain a quiescent phenotype, and store vitamin A under physiologic conditions. They undergo activation in response to inflammatory stimuli and become myofibroblastic cells [1, 2]. The latter phenotype secretes profibrogenic mediators, generates extracellular matrix materials, and thus plays a pivotal role in the fibrogenesis of the liver [3–5]. One of the features of activated HSC is their proliferation. An increase in the number of activated myofibroblasts together with the deposited extracellular matrix materials contributes to the formation of fibrotic septa forming C–C and P–C bridges. The suppression of HSC activation and cell number is thus a possible mechanism which can be exploited to establish therapeutic strategies against human liver fibrosis [6, 7].

Our previous studies have shown that antioxidative compounds, such as resveratrol and *N*-acetyl-L-cysteine exert anti-fibrotic activity in the liver and have an anti-proliferative effect on cultured HSC. [8–10]. Resveratrol functions as an inhibitor of tyrosine kinase and inhibits the phosphorylation of platelet-derived growth factor-receptor β (PDGFRβ) under PDGF-BB stimulation, leading to attenuation of the activation of mitogen-activated protein kinase (MAPK). *N*-acetyl-L-cysteine also inhibited DNA synthesis of cultured rat HSC stimulated by PDGF-BB through the cathepsin B-dependent proteolytic degeneration of PDGFRβ.

Recently, several clinical reports have revealed that interferon α (IFNα), especially when used in combination

with ribavirin, provides an effective therapy for chronic hepatitis C. Although the primary action of IFNα is to eradicate viruses, it has also been suggested to suppress and even cause the regression of liver fibrosis, as revealed by repeated liver biopsies performed in IFNα-treated patients with chronic hepatitis C [11, 12]. These reports strongly indicate that IFNα may induce the deactivation of human HSC, thereby reducing the septum-forming fibroblastic cell lineage. Herein, we show evidence for the anti-proliferative and pro-apoptotic actions of IFNα against human HSC [13].

Materials and methods

Materials

Recombinant PDGF-BB and tumor necrosis factor α (TNFα) were obtained from R&D Systems (Minneapolis, MO, USA). Polyclonal antibodies against extracellular signal-regulated kinases 1 and 2 (ERK1/2), phospho-ERK1/2 (Thr 202/Tyr 204), mitogen-activated kinase/ERK kinase (MEK), phospho-MEK, Akt, phospho-Akt (Ser 473), cytochrome c, caspase-3, and cleaved caspase-3 were purchased from Cell Signaling Technology, Inc. (Beverly, MA, USA) and those against cyclin D1, cdk2, cdk4, cdk6, p21, p27, p53, caspase-activated DNase (CAD), and inhibitor of CAD (ICAD) were acquired from Santa Cruz Biotechnology (Santa Cruz, CA, USA). Dulbecco's modified Eagle's medium (DMEM) and fetal bovine serum were purchased from Sigma Chemical Co. (Saint Louis, MO, USA). [^{3}H]Thymidine and enhanced chemiluminescence (ECL) detection reagent were purchased from Amersham Pharmacia Biotech (Buckinghamshire, England). Immobilon P membranes were purchased from Millipore Corp. (Bedford, MA, USA). Kodak XAR5 film was purchased from Eastman Kodak Co. (Rochester, NY, USA). Human natural IFNα was donated by Otsuka Pharmaceutical Co. (Tokushima, Japan). All other reagents were obtained from Sigma Chemical Co. or Wako Pure Chemical Co.

Preparation of human hepatic stellate cell line, LX-2

Human HSC-line, (LX-2, donated by Dr. Scott Friedman), a cell line spontaneously immortalized by growth in low serum, were established as previously reported. Characterizations of the cells were described in detail elsewhere [13]. Human HSC were maintained on plastic culture plates in DMEM supplemented with 10% fetal bovine serum. After the culture had continued for the indicated number of days, the medium was replaced by serum-free DMEM with test agents and the culture was continued for 48 h.

Immunoblot

Proteins were subjected to sodium dodecyl sulfate-polyacrylamide gel electrophoresis (SDS-PAGE) and then transferred to Immobilon P membranes. After blocking, the membranes were treated with primary antibodies followed by peroxidase-conjugated secondary antibodies. Immunoreactive bands were visualized using the enhanced chemiluminescence system (Amersham Pharmacia Biotech) and Kodak XAR5 film.

Cell growth assay

Subconfluent Human HSC-line was cultured on plastic dishes for 3 days in 10% FBS/DMEM, and then maintained for 24 h in serum-free DMEM. These cells were successively stimulated with test agents for 24 h, and then were pulse-labeled with 1.0 μCi/ml of [^{3}H]thymidine during the last 24 h. The incorporated radioactivity was counted by liquid scintillation, as previously described [9].

Cell survival assay

Cell survival was measured using the Alamar blue assay (BIOSOURCE) according to the manufacturer's instructions. In brief, 20 μl of Alamar blue was added to 6-well plates containing DMEM. Absorbance at 530 nm was measured using a micro-plate reader (Wallac 1420 ARVOsx, P-E Applied Biosystems).

DNA fragmentation assay

Cell samples were homogenized and centrifuged. The pellet was resuspended in 1 ml of lysis buffer consisting of 10 mmol/l Tris-HCl, pH 7.4, 10 mmol/l NaCl, 10 mmol/l ethylenediaminetetraacetic acid (EDTA), 100 g/l proteinase K, and 0.5% SDS and incubated for 2 h at 50°C before being treated with ribonuclease overnight at 37°C. After extraction with phenol–chloroform twice and precipitation with ethanol, the DNA was dissolved in TE buffer (10 mmol/l Tris-HCl, pH 7.5, 1 mmol/l EDTA). The DNA was loaded onto 1.5% agarose gel containing ethidium bromide, electrophoresed in Tris acetate/EDTA buffer for 2 h at 50 V, and photographed under ultraviolet illumination.

Flow cytometric quantification of apoptotic and necrotic cells

For quantification of apoptotic cells, we used flow cytometry (FACS Calibur HG; BD, Franklin Lakes, NJ) after trypsination of human HSC treated with IFNα or TNFα, IFNα/TNFα under serum-reduced conditions (0.1% FBS)

for 48 h [14]. To detect early apoptotic changes, staining with Annexin V-FITC, which is known to have high affinity to phosphatidylserine, and propidiumiodide were used according to the manufacturer's instructions (Roche Diagnostics, Rotkreuz, Switzerland).

Mitochondria/cytosol fractionation

Human HSC were treated with mediums supplemented with TNFα and/or IFNα for 24 h. Then, the cells were collected using a cell scraper, and the collected cells were pelleted by centrifugation at $600 \times g$ for 5 min at 4°C. After washing with ice-cold PBS, fractions with enriched mitochondria and cytosol were obtained using a Mitochondria/Cytosol fractionation kit (Bio Vision Research Products, Mountain View, CA, USA) according to the manufacturer's instructions. Individual fractions were stored at −80°C until use.

Statistical analysis

Data presented as bar graphs are the means ± S.D. of at least three independent experiments. Statistical analysis was performed using Student's *t*-test ($P < 0.01$ was considered significant).

Results

Effect of IFNα on DNA synthesis of human HSC-line

As shown in Fig. 1, human HSC incorporated 11 ± 2 (DPM × 10^4) of [^{3}H]thymidine in the presence of serum. DNA synthesis dose dependently decreased in the presence of IFNα; it decreased significantly to 71 and 48% of the control in the presence of 10^2 and 10^3 IU/ml, respectively, of IFNα. PDGF-BB (10 ng/ml) augmented DNA synthesis of HSC at about 1.2 times. Even in this condition, IFNα at a concentration of more than 10^3 IU/ml significantly suppressed DNA synthesis of HSC (Fig. 2).

Effect of IFNα on cell cycle-related protein expression and PDGF-BB-stimulated signal transduction in HSC

Because IFNα suppressed DNA synthesis of human HSC, we hypothesized that IFNα regulates cell cycle-related protein expression, thereby hampering cell cycle transition from the G1 to S phase. Thus, the expression of several cell cycle-related proteins was determined by immunoblot. As shown in Fig. 3a, the amount of major cell cycle-related proteins such as cyclin D1, cdk2, cdk4, cdk6, p21, and p27 was not affected by IFNα. Although a previous report using hepatoma cell lines indicated that p53 is involved in growth

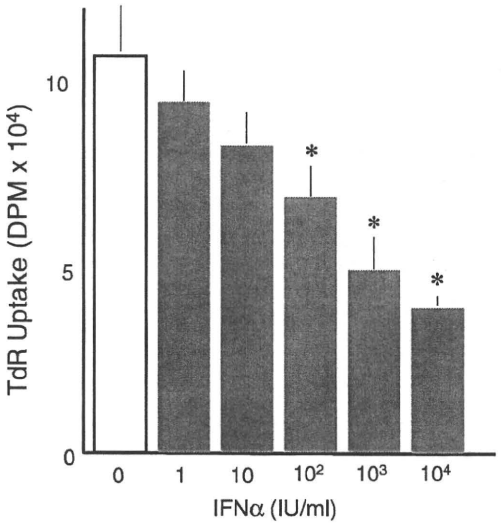

Fig. 1 Effect of IFNα on [^{3}H]thymidine incorporation in HSC. Sub-confluent HSC were cultured on plastic dishes for 3 days in 10% FBS/DMEM, and then maintained for 24 h in serum-free DMEM. These cells were successively stimulated with IFNα for 24 h, and then pulse-labeled with 1.0 μCi/ml of [^{3}H]thymidine during the last 24 h. The incorporated radioactivity was counted by liquid scintillation. $*P < 0.01$

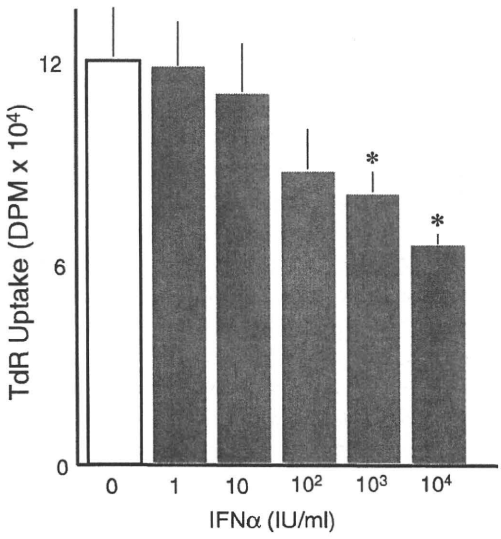

Fig. 2 Effect of IFNα on PDGF-BB-stimulated [^{3}H]thymidine incorporation in HSC. Sub-confluent HSC were cultured on plastic dishes for 3 days in 10% FBS/DMEM, and then maintained for 24 h in serum-free DMEM. These cells were successively stimulated with PDGF-BB (10 ng/ml) in the presence or absence of IFNα for 24 h, and then were pulse-labeled with 1.0 μCi/ml of [^{3}H]thymidine during the last 24 h. The incorporated radioactivity was counted by liquid scintillation. $*P < 0.01$

suppression by IFNα [15], we failed to observe the suppression of p53 in HSC treated with IFNα. The PDGF-BB-activated MEK-MAPK cascade and Akt were also unaffected (Fig. 3b).

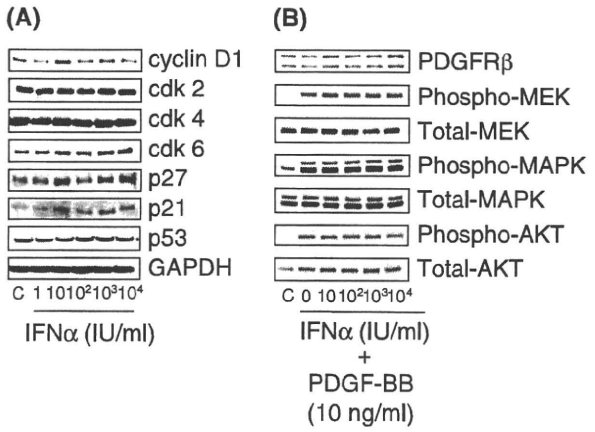

Fig. 3 Effects of IFNα on cell cycle-related protein expression and the activation of MEK, MAPK, and Akt stimulated with PDGF-BB in HSC. (**a**) Expression of cyclin D1, cdk2, cdk4, cdk6, p27, p21, and p53 was determined by immunoblot. (**b**) Expression of PDGFRβ, phospho-MEK, total MEK, phospho-MAPK, total MAPK, phospho-Akt, and total Akt in HSC under PDGF-BB (10 ng/ml) stimulation was analyzed by immunoblot

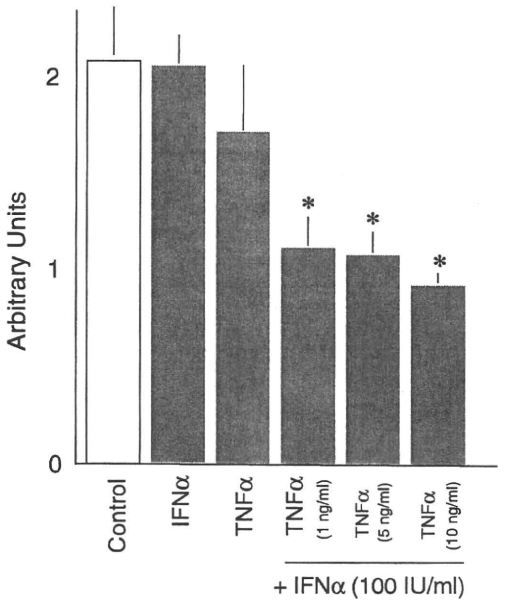

Fig. 4 Effect of IFNα and TNFα on number of HSC. HSC were maintained on plastic culture plates in DMEM supplemented with 10% fetal bovine serum. Then, the medium was replaced by serum-free DMEM with IFNα and/or TNFα and the culture was continued for another 48 h. Numbers of HSC were determined by the Alamar blue assay (BIOSOURCE) according to the manufacturer's instructions. $^*P < 0.01$

Induction of apoptosis of HSC by IFNα

Although the mechanism of IFNα-dependent DNA synthesis inhibition was not clear, we found that IFNα triggered the apoptosis of human HSC-line in the presence of a low dose of TNFα. As shown in Fig. 4, IFNα or TNFα alone failed to affect the number of HSC, as determined by the Alamar blue assay. However, the simultaneous addition of IFNα and TNFα significantly decreased the cell number to 54% of the control. In fact, when observed under a phase-contrast microscope, the cell density of human HSC became sparse when cells were treated with IFNα and TNFα for 48 h (Fig. 5). This finding indicates that cell death is actively stimulated by the combination of IFNα and TNFα. This observation was further supported by the fact that cell treatment with IFNα plus TNFα-induced DNA ladder formation (Fig. 6) and analysis using flow cytometric quantification of apoptosis of human HSC line (Fig. 7).

Role of IFNα on caspase cascade

Finally, we tested whether IFNα regulates the caspase cascade in human HSC-line. As shown in Fig. 8a, cytochrome c release from mitochondria into the cytosol was augmented by TNFα alone and TNFα/IFNα treatment. In accordance with this result, cleaved caspase 3 was enriched in cells treated with TNFα alone and TNFα/IFNα (Fig. 8b). Because TNFα alone thus triggered cytochrome c release and the activation of caspase 3 and failed to induce the active apoptosis of HSC, we hypothesized that IFNα may play a critical role in finalizing DNA fragmentation. After searching for the mechanism, we found that IFNα significantly reduced the level of ICAD without affecting the amount of CAD (Fig. 8c).

Discussion

IFNα is now a first-choice therapy for chronic hepatitis C (CH–C). In combination with rivabirin, IFN therapy leads to about a 30% and 80% eradication of HCV genotypes 1 and 2, respectively. Recently, pegylated IFNα has improved the efficacy of antiviral therapy [16, 17]. IFNα as well as IFNβ binds to cell surface receptors composed of IFNAR1 and IFNAR2 subunits. IFNα binding leads to ligand-induced receptor dimerization and then to the auto- and trans-phosphorylation of Janus protein tyrosine kinases, which successively induces the phosphorylation of STAT1/STAT2. Phosphorylated STAT1/STAT2 binds to IFN regulatory factor 9 (IRF-9) to form IFN-stimulated gene factor 3 (ISGF3), which translocates into the nucleus and binds to the IFN-stimulated response element (ISRE), initiating the transcription of IFN-dependent genes such as 2′-5′-oligoadenylate synthetase. These IFN-induced intracellular signalings suppress viral replication to complete viral eradication [18, 19].

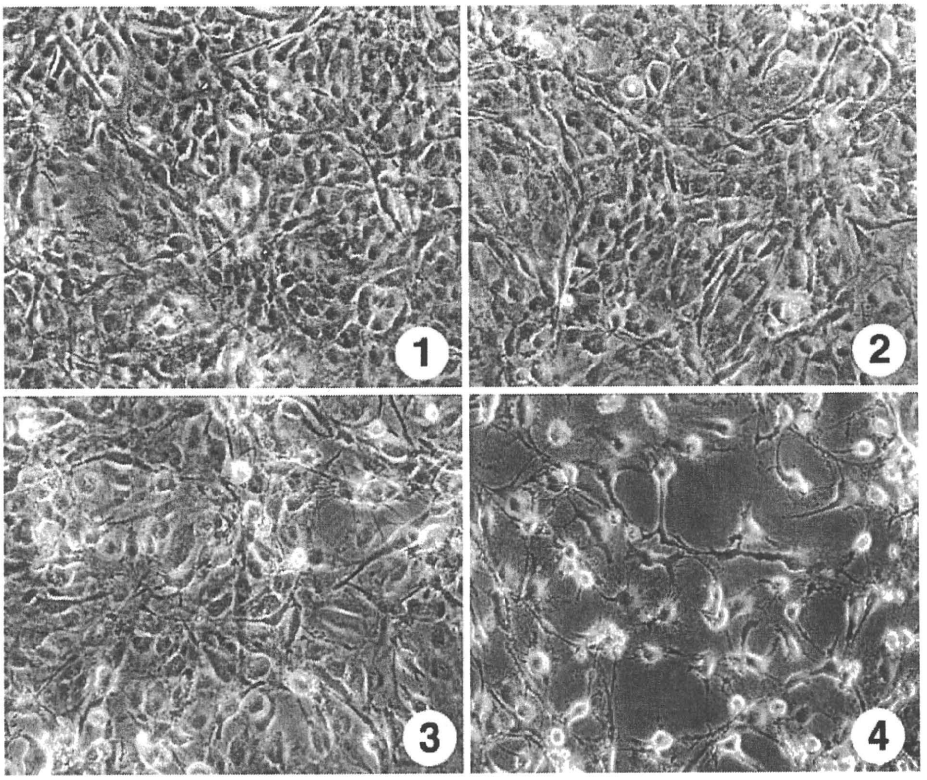

Fig. 5 Effect of IFNα and TNFα on the cell number of HSC. HSC were maintained on plastic culture plates in DMEM supplemented with 10% fetal bovine serum. Then, the medium was replaced by serum-free DMEM with IFNα and/or TNFα and the culture was continued for another 48 h. Cell appearance of HSC were determined under a microscope at a magnification of ×200. 1: Control; 2: IFNα; 3: TNFα; 4: IFNα/TNFα. Note that the cell number was markedly decreased by incubating them with IFNα plus TNFα. IFNα: 100 IU/ml. TNFα: 10 ng/ml

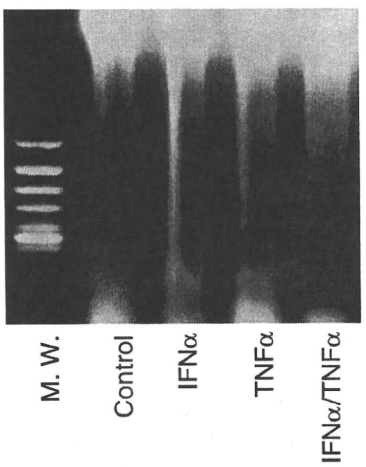

Fig. 6 DNA fragmentation of HSC treated with IFNα and TNFα. Isolated DNA was loaded onto a 1.5% agarose gel containing ethidium bromide, electrophoresed in Tris acetate/EDTA buffer for 2 h at 50 V, and photographed under ultraviolet illumination. Note that treatment of HSC with IFNα plus TNFα induced DNA flagmentation. IFNα: 100 IU/ml. TNFα: 10 ng/ml. M. W.: molecular weight

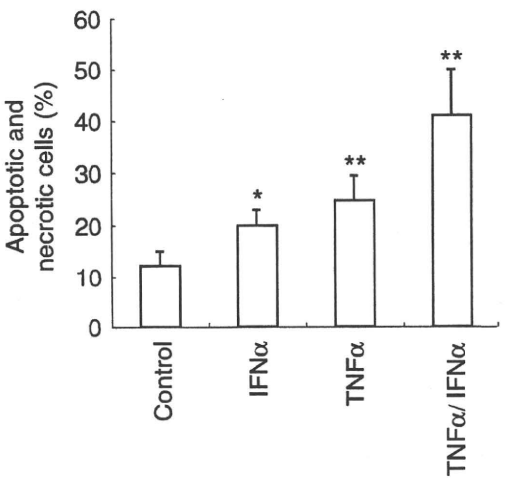

Fig. 7 Flow cytometric quantification of apoptosis in LX-2 treated with IFNα or TNFα, IFNα/TNFα. LX-2 cells were maintained on plastic culture plates in DMEM supplemented with 10% FBS. Then, the medium was replaced by serum-free DMEM with IFNα and/or TNFα and the culture was continued for another 48 h. The data show the percentile portion of apoptotic cells per total LX-2 population using flow cytometry. $*P < 0.05$; $**P < 0.01$

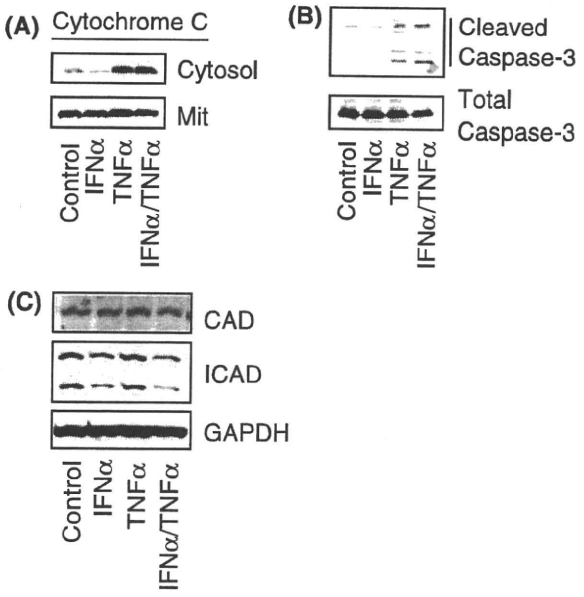

Fig. 8 Apoptosis-related protein expressions in HSC. (**a**) The cytochrome c content in the cytosol and mitochondria was determined by Western blot. (**b**) The activation of caspase-3 was studied by detecting the amount of cleaved caspase-3. (**c**) Expression of CAD and ICAD in HSC treated with IFNα and/or TNFα. IFNα: 100 IU/ml. TNFα: 10 ng/ml

In addition to the antiviral effect, IFNα is also known as a negative growth factor and shows anti-oncogenic activity [14]. Several lines of evidence have revealed that IFN therapy for CH–C lowers the occurrence of hepatocellular carcinoma (HCC), although the precise molecular mechanism has not yet been elucidated [20–22]. In addition, treatment using IFN in combination with 5′-fluorouracil (5-FU) was reported to be effective for advanced HCC with portal vein thrombosis [23, 24]. It has recently been reported that IFNα/β induces p53 gene transcription and increases the p53 protein level in HepG2 and HLE cells, two human hepatic cancer cell lines, thereby contributing to tumor suppression. However, the effect of IFN on the proliferation and cell survival of hepatic non-parenchymal collagen-producing HSCs has yet to be fully elucidated.

Several lines of evidence show that IFNα treatment for chronic hepatitis C leads to the regression of liver fibrosis even if HCV is not successfully eradicated [11, 12]. This fact indicates that IFNα has a direct anti-fibrotic action, most likely through its action against HSC. Initially, IFNγ was reported to successfully inhibit HSC activation, as revealed by its inhibitory effect on collagen synthesis and smooth muscle α-actin expression [25, 26]. Its in vivo anti-fibrotic action has also been elucidated [27, 28]. Successively, IFNα was proven to inhibit DNA synthesis of human HSC although a relatively weak inhibitory effect was seen at a concentration above 10^4 U/ml [29]. In the present study, we observed an almost 100-times stronger anti-proliferative effect using OIF, a natural IFNα. This discrepancy may be derived from the difference in IFN used and from the condition and culture system of HSC. Furthermore, in that report, Mallat et al. showed that IFNα suppressed [^{3}H]thymidine incorporation of human HSC stimulated with 5% fetal calf serum, PDGF-BB (20 ng/ml), PDGF-AA (20 ng/ml), or TGFβ1 (0.5 ng/ml), and that IFNα reduced the number of HSC stimulated with 5% fetal calf serum. However, the authors did not refer to the mechanism, especially to the induction of apoptosis of human HSC exposed to IFNα. Although we failed to clarify the mechanism of IFNα-dependent inhibition of cell cycle progression in human HSC-line, we found that natural IFNα contributes to the induction of apoptosis of human HSC by activating the caspase cascade, which provides a novel insight into the fibrosis regression in patients treated with IFNα derivatives.

Mallat et al. [29] additionally showed that IFNα as well as IFNγ reduced the secretion of prolines and the mRNA expressions of collagens α1(I) and α1(III). With respect to this mechanism, Inagaki et al. [30] recently reported that IFNα blocked promoter activation and prevented the progression of liver fibrosis induced by CCl_4 injection when administered to transgenic mice harboring the α2(I) collagen gene (COL1A2) promoter sequence, and that, in transient transfection assays, IFNα decreased the steady-state levels of COL1A2 mRNA and inhibited TGFβ/Smad3-stimulated COL1A2 transcription.

In addition to these previous observations, we herein found that IFNα in combination with a small amount of TNFα shows a pro-apoptotic effect in HSC. This effect is considered to be related to cytochrome c release into the cytosol from mitochondria and caspase-3 activation and be regulated by ICAD (Fig. 7). Although human HSC have been proven to be resistant to apoptosis [31], the data shown here clearly indicate that they undergo apoptosis at inflammatory liver sites in the presence of IFNα, which may at least partially account for the regression of liver fibrosis during IFN therapy due to chronic hepatitis C.

In conclusion, the present study demonstrates the anti-proliferative and pro-apoptotic actions of natural human IFNα against human HSC-line, and provides useful information regarding the mechanism of IFN-dependent regression of human liver fibrosis caused by viral infection.

Acknowledgments We thank Drs. Kazuki Nakatani, Naoto Maeda, Yukihiro Imanishi, and Koji Kinoshita for their critical comments on this work. This work was supported by a Grant-in-Aid for Scientific Research from the Japan Society for the Promotion of Science (JSPS). A part of this study was presented at the 12th International Symposium on Cells of the Hepatic Sinusoid (12th ISCHS).

References

1. Okuyama H, Shimahara Y, Kawada N. The hepatic stellate cell in the post-genomic era. Histol Histopathol 2002;17:487–495
2. Eng FJ, Friedman SL, Fibrogenesis I. New insights into hepatic stellate cell activation: the simple becomes complex. Am J Physiol Gastrointest Liver Physiol 2000;279:G7–G11
3. Friedman SL. Molecular regulation of hepatic fibrosis, an integrated cellular response to tissue injury. J Biol Chem 2000;275:2247–2250. doi:10.1074/jbc.275.4.2247
4. Gabele E, Brenner DA, Rippe DA. Liver fibrosis: signals leading to the amplification of the fibrogenic hepatic stellate cell. Front Biosci 2003;8:D69–D77. doi:10.2741/887
5. Pinzani M, Marra F. Cytokine receptors and signaling in hepatic stellate cells. Semin Liver Dis 2001;21:397–416. doi:10.1055/s-2001-17554
6. Albanis E, Friedman SL. Hepatic fibrosis. Pathogenesis and principles of therapy. Clin Liver Dis 2001;5:315–334. doi:10.1016/S1089-3261(05)70168-9
7. Bataller R, Brenner DA. Hepatic stellate cells as a target for the treatment of liver fibrosis. Semin Liver Dis 2001;21:437–451. doi:10.1055/s-2001-17558
8. Kawada N, Seki S, Inoue M, Kuroki T. Effect of antioxidants, resveratrol, quercetin, and N-acetylcysteine, on the functions of cultured rat hepatic stellate cells and Kupffer cells. Hepatology 1998;27:1265–1274. doi:10.1002/hep.510270512
9. Okuyama H, Shimahara Y, Kawada N, Seki S, Kristensen DB, Yoshizato K, et al. Regulation of cell growth by redox-mediated extracellular proteolysis of platelet-derived growth factor receptor beta. J Biol Chem 2001;276:28274–28280. doi:10.1074/jbc.M102995200
10. Matsui H, Ikeda K, Nakajima Y, Horikawa S, Kawada N. Sulfur-containing amino acids attenuate the development of liver fibrosis in rats through down-regulating stellate cell activation. J Hepatol 2004;40:917–925. doi:10.1016/S0168-8278(04)00065-0
11. Shiratori Y, Imazeki F, Moriyama M, Yano M, Arakawa Y, Yokosuka O, et al. Histologic improvement of fibrosis in patients with hepatitis C who have sustained response to interferon therapy. Ann Intern Med 2000;132:517–524
12. Poynard T, McHutchison J, Davis GL, Esteban-Mur R, Goodman Z, Bedossa P, et al. Impact of interferon alfa-2b and ribavirin on progression of liver fibrosis in patients with chronic hepatitis C. Hepatology 2000;32:1131–1137. doi:10.1053/jhep.2000.19347
13. Xu L, Hui AY, Albanis E, Arthur MJ, O'Byrne SM, Blaner WS, et al. Human hepatic stellate cell lines, LX-1 and LX-2: new tools for analysis of hepatic fibrosis. Gut 2005;54:142–151. doi:10.1136/gut.2004.042127
14. Saile B, Matthes N, Knittel T, Ramadori G. Transforming growth factor beta and tumor necrosis factor alpha inhibit both apoptosis and proliferation of activated rat hepatic stellate cells. Hepatology 1999;30:196–202. doi:10.1002/hep.510300144
15. Takaoka A, Hayakawa S, Yanai H, Stoiber D, Negishi H, Kikuchi H, et al. Integration of interferon-alpha/beta signalling to p53 responses in tumour suppression and antiviral defence. Nature 2003;424:516–523. doi:10.1038/nature01850
16. Hadziyannis SJ, Sette H Jr, Morgan TR, Balan V, Diago M, Marcellin P, et al. PEGASYS International Study Group. Peginterferon-alpha2a and ribavirin combination therapy in chronic hepatitis C: a randomized study of treatment duration and ribavirin dose. Ann Intern Med 2004;140:346–355
17. Manns MP, Wedemeyer H, Cornberg M. Treating viral hepatitis C: efficacy, side effects, and complications. Gut 2006;55:1350–1359. doi:10.1136/gut.2005.076646
18. Hoofnagle JH, Seeff LB. Peginterferon and ribavirin for chronic hepatitis C. N Engl J Med 2006;355:2444–2451. doi:10.1056/NEJMct061675
19. Gale M Jr, Foy EM. Evasion of intracellular host defence by hepatitis C virus. Nature 2005;436:939–945. doi:10.1038/nature04078
20. Nishiguchi S, Shiomi S, Nakatani S, Takeda T, Fukuda K, Tamori A, et al. Prevention of hepatocellular carcinoma in patients with chronic active hepatitis C and cirrhosis. Lancet 2001;357:196–197. doi:10.1016/S0140-6736(00)03595-9
21. Yoshida H, Arakawa Y, Sata M, Nishiguchi S, Yano M, Fujiyama S, et al. Interferon therapy prolonged life expectancy among chronic hepatitis C patients. Gastroenterology 2002;123:483–491. doi:10.1053/gast.2002.34785
22. Shiratori Y, Ito Y, Yokosuka O, Imazeki F, Nakata R, Tanaka N, et al. Tokyo-Chiba Hepatitis Research Group. Antiviral therapy for cirrhotic hepatitis C: association with reduced hepatocellular carcinoma development and improved survival. Ann Intern Med 2005;142:105–114
23. Kondo M, Nagano H, Wada H, Damdinsuren B, Yamamoto H, Hiraoka N, et al. Combination of IFN-alpha and 5-fluorouracil induces apoptosis through IFN-alpha/beta receptor in human hepatocellular carcinoma cells. Clin Cancer Res 2005;11:1277–1286. doi:10.1158/1078-0432.CCR-05-0274
24. Eguchi H, Nagano H, Yamamoto H, Miyamoto A, Kondo M, Dono K, et al. Augmentation of antitumor activity of 5-fluorouracil by interferon alpha is associated with up-regulation of p27Kip1 in human hepatocellular carcinoma cells. Clin Cancer Res 2000;6:2881–2890
25. Tiggelman AM, Boers W, Linthorst C, Sala M, Chamuleau RA. Collagen synthesis by human liver (myo)fibroblasts in culture: evidence for a regulatory role of IL-1 beta, IL-4, TGF beta and IFN gamma. J Hepatol 1995;23:307–317
26. Rockey DC, Maher JJ, Jarnagin WR, Gabbiani G, Friedman SL. Inhibition of rat hepatic lipocyte activation in culture by interferon-gamma. Hepatology 1992;16:776–784. doi:10.1002/hep.1840160325
27. Sakaida I, Uchida K, Matsumura Y, Okita K. Interferon gamma treatment prevents procollagen gene expression without affecting transforming growth factor-beta1 expression in pig serum-induced rat liver fibrosis in vivo. J Hepatol 1998;28:471–479. doi:10.1016/S0168-8278(98)80322-X
28. Baroni GS, D'Ambrosio L, Curto P, Casini A, Mancini R, Jezequel AM, et al. Interferon gamma decreases hepatic stellate cell activation and extracellular matrix deposition in rat liver fibrosis. Hepatology 1996;23:1189–1199. doi:10.1002/hep.510230538
29. Mallat A, Preaux AM, Blazejewski S, Rosenbaum J, Dhumeaux D, Mavier P. Interferon alfa and gamma inhibit proliferation and collagen synthesis of human Ito cells in culture. Hepatology 1995;21:1003–1010
30. Inagaki Y, Nemoto T, Kushida M, Sheng Y, Higashi K, Ikeda K, et al. Interferon alfa down-regulates collagen gene transcription and suppresses experimental hepatic fibrosis in mice. Hepatology 2003;38:890–899
31. Novo E, Marra F, Zamara E, Valfre di Bonzo L, Monitillo L, Cannito S, et al. Overexpression of Bcl-2 by activated human hepatic stellate cells: resistance to apoptosis as a mechanism of progressive hepatic fibrogenesis in humans. Gut 2006;55:1174–1182. doi:10.1136/gut.2005.082701

Journal of Medical Virology 81:1009–1014 (2009)

Frequent Detection of Hepatitis B Virus DNA in Hepatocellular Carcinoma of Patients With Sustained Virologic Response for Hepatitis C Virus

Akihiro Tamori,[1]* Takehiro Hayashi,[1] Mayumi Shinzaki,[1] Sawako Kobayashi,[1] Shuji Iwai,[1] Masaru Enomoto,[1] Hiroyasu Morikawa,[1] Hiroki Sakaguchi,[1] Susumu Shiomi,[2] Shigekazu Takemura,[3] Shoji Kubo,[3] and Norifumi Kawada[1]

[1]*Department of Hepatology, Osaka City University Graduate School of Medicine, Osaka, Japan*
[2]*Department of Nuclear Medicine, Osaka City University Graduate School of Medicine, Osaka, Japan*
[3]*Department of Surgery, Osaka City University Graduate School of Medicine, Osaka, Japan*

Hepatocellular carcinoma (HCC) develops several years after the eradication of hepatitis C virus (HCV) by interferon therapy. Risk factors for the development of HCC are only partly understood. To elucidate the role of occult hepatitis B virus (HBV) infection in hepatocarcinogenesis in patients with sustained virologic response, the prevalences of HBV-related makers were examined. Study group comprised 16 patients with sustained virologic response (group A) and 50 with HCV (group B). Anti-HBc and anti-HBs in serum were examined by enzyme-linked immunoassay. HBV DNA in liver was examined by nested polymerase chain reaction, using primers specific for genes encoding for HBx, HBsAg, HBcAg, and HBV cccDNA. Sequence of the amplified HBV DNA for 'a' determinant of HBsAg was determined in HCC. Anti-HBc was positive in 10 of 16 in group A and 25 of 50 in group B. HBV DNA in liver was detected in 12 of 16 in group A and 21 of 50 in group B ($P = 0.044$). In group A, HBV DNA in liver was detected frequently in patients without cirrhosis and in those with a longer period from the time of HCV eradication to the development of HCC. Mutation in 'a' determinant of HBsAg was found in three HCC of group A. Occult HBV infection may be one of the most important risk factors in hepatocarcinogenesis of Japanese patients with sustained virologic response. ***J. Med. Virol. 81:1009–1014, 2009.*** © 2009 Wiley-Liss, Inc.

KEY WORDS: anti-HBc; anti-HBs; interferon; occult HBV infection

INTRODUCTION

In Japan, a country endemic for hepatitis B virus (HBV) and hepatitis C virus (HCV), more than 75% of cases of hepatocellular carcinoma (HCC) are attributable to HCV-related chronic liver disease, and nearly 15% are attributable to HBV-related liver disease [Ikai et al., 2007]. Several reports have focused on the clinical role of past HBV infection as indicated by the presence of anti-HBc and the absence of HBsAg in patients with HCV. Marusawa et al. [1999] reported that the prevalence of anti-HBc was high in patients with chronic liver disease, especially in HCC associated with HCV. A retrospective study of 412 patients with HCV showed that the risk of hepatocarcinogenesis increased twofold in patients with anti-HBc [Chiba et al., 1996]. Prospective studies have also demonstrated that the presence of anti-HBc is an important risk factor for HCC in patients with HCV [Tanaka et al., 2006; Ikeda et al., 2007]. Conversely, some studies failed to support a role of previous HBV infection in hepatocarcinogenesis [Hiraoka et al., 2003; Stroffolini et al., 2008].

Another important clinical feature is occult HBV infection, defined as the presence of detectable levels of HBV DNA in liver despite the absence of serum hepatitis B surface antigen (HBsAg). The HBV genome is detectable frequently in liver tumors from HBsAg-negative patients with HCV-related liver disease, suggesting that occult HBV infection may contribute to the progression of liver damage and the development of HCC in HCV-positive patients [Cacciola et al., 1999; Tamori et al., 1999, 2003; Squadrito et al., 2006; Pollicino et al., 2004].

Interferon (IFN) has potent antiviral activity against HCV. Complete eradication of HCV by antiviral therapy is associated with a considerable reduction in the

*Correspondence to: Akihiro Tamori, Department of Hepatology, Osaka City University Graduate School of Medicine, 1-4-3 Asahimachi, Abeno-ku, Osaka 545-8585, Japan.
E-mail: atamori@med.osaka-cu.ac.jp

Accepted 10 February 2009
DOI 10.1002/jmv.21488
Published online in Wiley InterScience (www.interscience.wiley.com)

incidence of HCC [Yoshida et al., 1999; Tanaka et al., 2000]. Nevertheless, recent studies have shown that HCC develops in 2.5–4.2% of patients who have a sustained virologic response [Toyoda et al., 2000; Ikeda et al., 2005; Kobayashi et al., 2007]. These patients may have had advanced liver fibrosis at the time of HCV eradication, and subclinical tumors might already be present in the liver at the end of IFN therapy [Makiyama et al., 2004]. In some patients with sustained virologic response, however, HCC develops from liver without fibrosis several years after the eradication of HCV by IFN. The etiology of such cases of HCC remains obscure. Delineation of important features of HCC that develop after the elimination of HCV as compared with those established during sustained HCV infection may contribute to a better understanding of the mechanisms involved.

In the present study, resected liver specimens were examined to evaluate the role of previous and occult HBV infection in the development of cancer after the clearance of HCV by IFN treatment. The present results might contribute to a clearer definition of patients at high risk for HCC after the eradication of HCV.

MATERIALS AND METHODS

Patients

Sixteen consecutive patients who underwent surgical resection of HCC in Osaka City University Hospital after eradication of HCV by interferon monotherapy from June 1998 through July 2007 (group A) were studied (Table I). All patients with sustained virologic response were male in the present study. As a sex-matched control, 50 consecutive HCV-RNA-positive men with HCC during the same period were studied (group B). Serological markers showed that anti-HCV was positive and HBsAg was negative in all patients. One portion of each tissue sample from the 66 patients with HCC was frozen in liquid nitrogen immediately after resection and stored at −80°C until analysis. Total DNA was extracted from these portions by conventional methods as described previously [Tamori et al., 2003]. None of the patients had a history of exposure to aflatoxin B1, insulin administration, hereditary hemochromatosis, autoimmune hepatitis, or primary biliary cirrhosis. The activity of hepatitis and the stage of fibrosis were determined according to a modified version of Desmet's classification in liver tissue specimens obtained before IFN therapy and in noncancerous liver tissue obtained intraoperatively.

Anti-HBc and Anti-HBs in Serum

Antibodies to HBsAg (anti-HBs) and anti-HBc in patient sera were tested by enzyme immunoassay and/or radioimmunoassay, using commercially available kits (Dainabott, Tokyo, Japan).

Detection of HBV DNA in Serum and Liver

DNA was extracted from 100 μl of serum or 10 mg of liver tissue by phenol/chloroform extraction, as described previously [Tamori et al., 2003]. HBV DNA in serum or in liver was amplified with specific primers for genes encoding for HBx, HBsAg, and HBcAg (sequences of the primers shown in Table II). Amplification was done in a thermal cycler for 35 cycles: 95°C for 30 sec, 55°C for 60 sec, and 72°C for 60 sec in 40 μl of a reaction buffer containing 30 pmol of the two appropriate primers, four deoxynucleotides each at a concentration of 100 μM, polymerase chain reaction (PCR) buffer, and 2.5 units of Gold Taq polymerase (Perkin-Elmer Cetus, Norwalk, CT). The first PCR product (2 μl) was used in a second PCR. To examine HBV covalently closed circular DNA (cccDNA) in liver, extracted DNA

TABLE I. Clinical Characteristics of HCC-Patients With Sustained Virological Response and With HCV

	Group A: sustained virologic response	Group B: HCV	*P*-value
Patients, n	16	50	
Age	66.1 (55–79)	65.7 (55–76)	0.465
HBsAg (+/−)	0/16	0/50	
Anti-HBs (+/−)	6/10	9/41	0.201
Anti-HBc (+/−)	10/6	25/25	0.559
Anti-HCV (+/−)	16/0	50/0	
HCV RNA (+/−)	0/16	50/0	
Alcohol			
>30 g/day	0	6	
<30 g/day	6	20	
None	10	24	0.47
Diabetes melitus (+/−)	2/14	17/33	0.182
Hypertention (+/−)	7/9	18/32	0.795
BMI	24.1 (17.4–28.1)	23.0 (17.9–29.8)	0.188
Hepatic cirrhosis (+/−)	4/12	24/26	0.184
Tumor grades			
Well-d	0	5	
Moderately d	6	25	
Poorly d	10	20	0.199

BMI, body mass index, Well-d, well-differentiated HCC, Moderately d: moderately differentiated HCC, Poorly d: poorly differentiated HCC.

TABLE II. Primers Used for Amplification of HBV DNA

Forward primers		Reverse primers	
HBx-1: 1220–1239	5′-CTCTCTCGGAAATACACCTC	HBx-2: 1818–1799	5′-GTAACTCCACAGAAGCTCCA
HBx-3: 264-1293	5′-TGCCAACTGGATCCTGCGCGG-GACGTCCTT	HBx-4: 1742–1723	5′-GGCTTGAACAGTAGGACATG
HBs-1: 391–408	5′-AAGACCTGCACGATTCCT	HBs-2: 672–654	5′-TAGAGGTAAAAAGGGACTC
HBs-3: 499–517	5′-TTCGCAAGATTCCTATGGG	HBs-4: 634–617	5′-GCCCCCAATACCACATCA
HBc-1: 1690–1708	5′-AACTTTTTCACCTCTGCCT	HBc-2: 1945–1929	5′-GCTTGCCTGAGTGCTGT
HBc-3: 1731–1749	5′-ACTGTTCAAGCCTCCAAGC	HBc-4: 1848–1829	5′-AAGGAAAGAAGTCAGAAGGC
P23: 1443–1462	5′-CTGAATCCCGCGGACGACCC	P24: 1891–1871	5′-ACCCAAGGCACAGCTTGGAGG
P25: 1553–1573	5′-GTCTGTGCCTTCTCATCTGCC	P26: 1846–1823	5′-AGATGATTAGGCAGAGGT-GAAAAA
HBs'a'-1: 52–71	5′-CTAGGACCCCTGCTCGTGTT	HBs'a'-2: 545–526	5′-AGCCAGGAGAAACGGACTGA
HBs'a'-3: 69–89	5′-GTTACAGGCGGGGTTTTTCTT		

was amplified with primers P23, 24, 25, and p26 (Table II). The amplification procedure and primers have been described previously [Tamori et al., 2005]. The nested PCR analysis was sufficiently sensitive to detect more than 10 copies of HBV DNA [Yotsuyanagi et al. 2000]. Occult HBV infection was diagnosed when two or more regions of HBV DNA were amplified, as reported previously [Pollicino et al., 2004].

Sequence of 'a' Determinant of HBsAg and HBV Genotyping

HBV DNA in liver was amplified with specific primers for HBS 'a' determinant (sequences of the primers shown in Table II). PCR (an initial incubation at 94°C for 5 min, followed by 35 cycles of 94°C for 30 sec, 55°C for 30 sec, and 72°C for 1 min) was performed in a final volume of 50 μl with a GeneAmp PCR system 9600 (Perkin-Elmer Life Sciences Japan, Tokyo, Japan). Aberrant PCR products were purified with a QIAquick PCR purification kit (Qiagen, Tokyo, Japan) and sequenced with an Applied Biosystems DNA sequencer (Perkin-Elmer) and a Dye Terminator Cycle Sequencing FS Ready Reaction kit (Applied Biosystems, Tokyo, Japan). HBV genotyping in liver was performed by PCR using type-specific primers [Naito et al., 2001].

Statistical Analysis

Statistical analysis was performed with the Statview SE+Graphics program, version 5.0 (SAS Institute, Cary, NC). The Mann–Whitney *U*-test was used to compare two continuous variables, and the χ^2 test was used to compare two categorical variables. All tests was two-sided and P value <0.05 was considered to be statistically significant.

Ethical Considerations

This study protocol complied with the ethical guidelines of the Declaration of Helsinki (1975) and was approved by the Ethics Committee of Osaka City University Graduate School of Medicine.

RESULTS

Histological Findings in Patients With HCC

In group A, 4 patients (25%) had hepatic cirrhosis. In group B, 24 patients (48%) had hepatic cirrhosis. This difference was not significant. Table I shows the histological tumor grade in each group. There was no significant difference between the two groups.

In patients with sustained virologic response, the period from the end of IFN treatment to the diagnosis for HCC ranged from 13 to 177 months. Histological examinations before and after IFN treatment, performed in 11 of the 16 patients in group A, showed that the staging of hepatic fibrosis improved in 5 patients and the grade of hepatic activity improved in 10 patients (Table III). In noncancerous liver, there was no fat accumulation.

Anti-HBc, Anti-HBs, and HBV DNA in Serum

Anti-HBc was positive in 10 (62.5%) of 16 patients in group A and 25 (50%) of 50 patients in group B ($P = 0.56$). Anti-HBs was detected in 6 (37.5%) of 16 patients in group A and 9 (18%) of 50 patients in group B ($P = 0.2$). HBV DNA was not detected in serum from either patients in group A or those in group B.

HBV DNA in the Resected Liver

HBV DNA in the resected liver was found in 12 (75%) of 16 patients in group A and 21 (42%) of 50 in group B. The rate of HBV DNA detection was significantly higher in patients with sustained virologic response than in patients with HCV ($P = 0.044$).

In group A, HBV DNA was detected in 7 resected livers from 10 patients with anti-HBc and in 5 resected livers from 6 patients without anti-HBc.

Among patients in group A, HBV DNA was detected in 11 (92%) of 12 patients without cirrhosis and 1 (25%) of 4 patients with cirrhosis ($P = 0.046$). Among patients in group B, HBV DNA was detected in 11 (42%) of 26 patients without cirrhosis and in 10 (42%) of 24 patients with cirrhosis (Table IV).

TABLE III. Clinicopathological Data in HCC-Patients With Sustained Virologic Response

Case	Pre-IFN therapy				Period from HCV eradication to diagnosis of HCC	At operation	
	Genotype	Viral load	F factor	A factor		F factor	A factor
56	1b	1 Meq	2	2	45 months	2	1
101	2a	Unknown	3	2	19 months	4	2
149	2a	1.1 Meq	4	3	20 months	4	2
196	2b	Unknown	2	2	41 months	1	2
198	2a	0.4 Meq	2	2	103 months	1	1
200	2a	1.1 Meq	2	2	13 months	2	1
221	2a	0.9 Meq	2	3	80 months	2	2
268	Unknown	Unknown	Unknown	Unknown	144 months	1	1
269	2a	0.4 Meq	2	3	156 months	0	0
271	1b	Unknown	4	1	156 months	3	1
325	1b	300 KIU	3	2	15 months	2	1
327	2b	160 KIU	3	3	36 months	4	2
328	1b	Unknown	Unknown	Unknown	14 months	4	2
336	1b	100 KIU	2	2	152 months	2	0
340	1b	0.9 Meq	2	3	177 months	2	1
347	Unknown	Unknown	Unknown	Unknown	60 months	3	1

F factor is hepatic fibrosis score in the liver. A factor is hepatitis activity in the liver.

HBV cccDNA was detected in 5 (31%) of 16 patients in group A and in 7 (14%) of 50 patients in group B ($P = 0.24$).

Average of the period from the end of IFN treatment to the diagnosis of HCC was 94 months in patients with occult HBV infection and 22 months in those without occult HBV infection. In group A, HBV DNA was detected in all patients in whom HCC developed more than 40 months after the disappearance of HCV (Table IV).

Mutation of the 'a' Determinant of HBsAg and HBV Genotype in Patients With Sustained Virologic Response

In 6 of 12 patients with occult HBV infection, the 'a' determinant area of HBsAg was amplified. Sequencing of the PCR product showed that codon 126 ATT (Ile) had mutated to GTT (Val) in two cases. One of them had two mutations, which were TCG to TTG at codon 54 and GCT to GGT at codon 157. In the other case, TTC had mutated to TCT at codon 93. No other mutations in the 'a' determinant area were found. HBV genotyping was performed in 12 patients with occult HBV infection. Eight patients were infected with HBV genotype C. In the four other patients, the HBV genotype could not be determined.

DISCUSSION

Previous studies have reported that 43–59% of patients with HCC related to HCV are positive for anti-HBc [Marusawa et al., 1999; Ikeda et al., 2007; Stroffolini et al., 2008]. In the present study, anti-HBc and anti-HBs were detected respectively in 50% and 18% of 50 patients with HCV-HCC. As compared with patients who had HCV-HCC, anti-HBc and anti-HBs were detected more frequently in HCC-patients with

TABLE IV. Clinical Characteristics of HCC-Patients With Sustained Virologic Response and With HCV; Stratified According to Occult HBV Infection

	Sustained virologic response		HCV	
	With occult HBV	Without occult HBV	With occult HBV	Without occult HBV
N	12	4	21	29
Age	66.1	66.3	63.8	65.3
Cirrhosis/non-cirrhosis	1/11*	3/1*	10/11	14/15
Period from HCV eradication to diagnosis of HCC (months)	94** (14–177)	22** (13–36)	—	—
Alcohol				
>30 g/day	0	0	4	2
<30 g/day	5	1	5	15
None	7	3	12	12
Diabetes melitus (+/−)	2/10	0/4	5/16	12/17
Hypertension (+/−)	5/7	2/2	8/13	10/19
BMI	23.9	24.4	23.6	22.5

*$P = 0.046$.
**$P = 0.036$.

sustained virologic response. Recent studies show a higher prevalence of anti-HBc in HCC-patients with sustained virologic response [Ikeda et al., 2007; Stroffolini et al., 2008]. The results in the present study were consistent with these reports. The prevalence of anti-HBc is higher among the elderly population in Japan. In the present study, mean ages and age distributions did not significantly differ between the patients with sustained virologic response and the patients with HCV. Taken together, anti-HBc might be one of the specific characteristics of HCC-patients with sustained virologic response.

Occult HBV infection was diagnosed when HBsAg in serum was negative and HBV DNA in serum or liver was positive, irrespective of test results for serum anti-HBc. Previous studies showed a high prevalence of occult HBV infection in patients with HCV and progressive liver disease, particularly HCC [Cacciola et al., 1999; Tamori et al., 1999]. Another report suggested that occult HBV infection is an independent risk factor for carcinogenesis in patients with HCV [Pollicino et al., 2004]. It is controversial whether very small amounts of HBV have carcinogenic potential in patients with HCV. HBV DNA integration into the human genome, one of the most important mechanisms of HBV-related hepatocarcinogenesis [Bréchot, 2004], was suggested to accelerate tumor progression in HBsAg-negative patients with HCV infection [Tamori et al., 2003]. However, a recent study showed that the incidence of HCC in HBsAg-negative patients with HBV DNA integration was not higher than that in patients without such integration [Toyoda et al., 2008]. The role of HBV DNA integration in patients with HCV infection remains to be clarified. On the other hand, there are few reports about occult HBV infection in patients with HCC in whom HCV was eradicated by IFN treatment. The present study clearly showed that the detection rate for HBV DNA was significantly higher in HCC-patients with sustained virologic response than in HCC-patients with HCV. Stroffolini et al. [2008] speculated that the disappearance of HCV might up-regulate HBV replication later on. In the present study, HBV cccDNA essential for HBV replication was detected in the liver from patients with occult HBV infection. HBV cccDNA was detected in small amounts, but not significantly more frequently in patients with sustained virologic response than in patients with HCV. It was suggested that HBV is re-amplified or accumulated in the liver of HCC-patients with sustained virologic response. Although HBV DNA integration in HCC of patients with sustained virologic response has been confirmed [Tamori et al., 2005], further studies are needed to elucidate the precise role of occult HBV infection in patients with sustained virologic response.

In the present study, eight patients with occult HBV infection were infected with HBV genotype C. A previous study reported that 610 (84.7%) of 720 Japanese patients with chronic HBV infection had genotype C [Orito et al., 2001]. In Japan, genotype C is predominant in both patients with occult HBV infection and patients with HBsAg. It is speculated that occult HBV infection occurred after the disappearance of HBsAg in patients with HBV infection.

Mutation in 'a' determinant of HBsAg, which contributes to defective HBsAg expression [Chen and Oon, 1999], was detected in only three of 12 HCC with occult HBV infection. HBV DNA was not detected in serum from any patient in the present study. It appears that the 'a' determinant mutation does not have a major role in the pathogenesis of occult HBV infection in patients with sustained virologic response. Molecular analysis of the full-length HBV genome in patients with occult HBV infection has shown that viral factors are not responsible for the unique HBV status [Pollicino et al., 2007]. Available evidence suggests that small amounts of HBV, detected only in liver, exist without inducing hepatic injury or that HBV DNA is integrated into hepatocyte nuclei.

Previous studies in Japanese patients indicated that male sex, higher age, and advanced liver fibrosis before IFN therapy are risk factors for HCC in patients with sustained virologic response [Toyoda et al., 2000; Makiyama et al., 2004]. It has been suggested that subclinical tumors are most likely present in liver with severe fibrosis before HCV eradication. In the present study, however, histological findings before IFN therapy showed mild fibrosis (stage 2) in eight HCC-patients with sustained virologic response. In five patients, HCC was diagnosed more than 10 years after the eradication of HCV by IFN. It is doubtful whether neoplastic cells induced by HCV had existed in liver with milder fibrosis and proliferated slowly over such a long period. On the other hand, HBV DNA was detected frequently in HCC-patients without cirrhosis. In addition, HBV DNA was detected in HCC-patients with sustained virologic response that developed more than 40 months after HCV eradication. These results suggest that occult HBV infection is related to carcinogenesis in non-cirrhotic patients with sustained virologic response.

Recently, nonalcoholic steatohepatitis (NASH) is one of the causes of underlying non-viral hepatic cirrhosis and cryptogenic HCC. At the onset of HCC in patients with steatohepatitis, the noncancerous liver is often cirrhotic. In the present study, the noncancerous liver was not cirrhotic in 12 of 16 HCC-patients with sustained virologic response. The frequency of obesity, diabetes mellitus, and alcohol intake, factors related to steatohepatitis, in HCC patients with sustained virologic response were similar to those in HCC-patients with HCV. These findings suggest that steatohepatitis was not a major risk factor for HCC in patients with sustained virologic response.

In the present retrospective study, HBV DNA in liver was detected frequently in HCC of patients with sustained virologic response compared to in HCV-HCC. On the other hand, a follow up study for 15 patients with sustained virologic response showed that HBV DNA in liver was not detected in two patients in which HCC developed [Tsuda et al., 2004]. However, the number of examined patients in this report was small. A

large scale of prospective study is necessary to define the role of occult HBV infection on hepatocarcinogenesis in patients with sustained virologic response.

In conclusion, the above findings provide compelling evidence that continuous existence of HBV DNA in liver may be one of the risk factors for the development of HCC in patients with sustained virologic response in Japan.

ACKNOWLEDGMENTS

The authors thank Dr. Le Thi Thanh Thuy for excellent technique. Also, the authors thank Prof. Shuhei Nishiguchi, Department of Internal Medicine, Hyogo College of Medicine, for his advice and comments.

REFERENCES

Bréchot C. 2004. Pathogenesis of hepatitis B virus-related hepatocellular carcinoma: Old and new paradigms. Gastroenterology 127:S56–S61.

Cacciola I, Pollicino T, Squadrito G, Cerenzia G, Orlando ME, Raimondo G. 1999. Occult hepatitis B virus infection in patients with chronic hepatitis C liver disease. N Engl J Med 341:22–26.

Chen WN, Oon CJ. 1999. Human hepatitis B virus mutants: Significance of molecular changes. FEBS Lett 453:237–242.

Chiba T, Matsuzaki Y, Abei M, Shoda J, Tanaka N, Osuga T, Aikawa T. 1996. The role of previous hepatitis B virus infection and heavy smoking in hepatitis C virus-related hepatocellular carcinoma. Am J Gastroenterol 91:1195–1203.

Hiraoka T, Katayama K, Tanaka J, Ohno N, Joko K, Komiya Y, Kumagai J, Mizui M, Hino K, Miyakawa Y, Yoshizawa H. 2003. Lack of epidemiological evidence for a role of resolved hepatitis B virus infection in hepatocarcinogenesis in patients infected with hepatitis C virus in Japan. Intervirology 46:171–176.

Ikai I, Arii S, Okazaki M, Okita K, Omata M, Kojiro M, Takayasu K, Nakanuma Y, Makuuchi M, Matsuyama Y, Monden M, Kudo M. 2007. Report of the 17th Nationwide Follow-up Survey of Primary Liver Cancer in Japan. Hepatol Res 37:676–691.

Ikeda M, Fujiyama S, Tanaka M, Sata M, Ide T, Yatsuhashi H, Watanabe H. 2005. Risk factors for development of hepatocellular carcinoma in patients with chronic hepatitis C after sustained response to interferon. J Gastroenterol 40:148–156.

Ikeda K, Marusawa H, Osaki Y, Nakamura T, Kitajima N, Yamashita Y, Kudo M, Sato T, Chiba T. 2007. Antibody to hepatitis B core antigen and risk for hepatitis C-related hepatocellular carcinoma: A prospective study. Ann Intern Med 146:649–656.

Kobayashi S, Takeda T, Enomoto M, Tamori A, Kawada N, Habu D, Sakaguchi H, Kuroda T, Kioka K, Kim SR, Kanno T, Ueda T, Hirano M, Fujimoto S, Jomura H, Nishiguchi S, Seki S. 2007. Development of hepatocellular carcinoma in patients with chronic hepatitis C who had a sustained virological response to interferon therapy: A multicenter, retrospective cohort study of 1124 patients. Liver Int 27:186–191.

Makiyama A, Itoh Y, Kasahara A, Imai Y, Kawata S, Yoshioka K, Tsubouchi H, Kiyosawa K, Kakumu S, Okita K, Hayashi N, Okanoue T. 2004. Characteristics of patients with chronic hepatitis C who develop hepatocellular carcinoma after a sustained response to interferon therapy. Cancer 101:1616–1622.

Marusawa H, Osaki Y, Kimura T, Ito K, Yamashita Y, Eguchi T, Kudo M, Yamamoto Y, Kojima H, Seno H, Moriyasu F, Chiba T. 1999. High prevalence of anti-hepatitis B virus serological markers in patients with hepatitis C virus related chronic liver disease in Japan. Gut 45:284–288.

Naito H, Hayashi S, Abe K. 2001. Rapid and specific genotyping system for hepatitis B virus corresponding to six major genotypes by PCR using type-specific primers. J Clin Microbiol 39:362–364.

Orito E, Ichida T, Sakugawa H, Sata M, Horiike N, Hino K, Okita K, Okanoue T, Iino S, Tanaka E, Suzuki K, Watanabe H, Hige S, Mizokami M. 2001. Geographic distribution of hepatitis B virus (HBV) genotype in patients with chronic HBV infection in Japan. Hepatology 34:590–594.

Pollicino T, Squadrito G, Cerenzia G, Cacciola I, Raffa G, Craxi A, Farinati F, Missale G, Smedile A, Tiribelli C, Villa E, Raimondo G. 2004. Hepatitis B virus maintains its pro-oncogenic properties in the case of occult HBV infection. Gastroenterology 126:102–110.

Pollicino T, Raffa G, Costantino L, Lisa A, Campello C, Squadrito G, Levrero M, Raimondo G. 2007. Molecular and functional analysis of occult hepatitis B virus isolates from patients with hepatocellular carcinoma. Hepatology 45:277–285.

Squadrito G, Pollicino T, Cacciola I, Caccamo G, Villari D, La Masa T, Restuccia T, Cucinotta E, Scisca C, Magazzu D, Raimondo G. 2006. Occult hepatitis B virus infection is associated with the development of hepatocellular carcinoma in chronic hepatitis C patients. Cancer 106:1326–1330.

Stroffolini T, Almasio PL, Persico M, Bollani S, Benvegnù L, Di Costanzo G, Pastore G, Aghemo A, Stornaiuolo G, Mangia A, Andreone P, Stanzione M, Mazzella G, Saracco G, Del Poggio P, Bruno S, On behalf of Italian Association of the Study of the Liver Disease (AISF). 2008. Lack of correlation between serum anti-HBcore detectability and hepatocellular carcinoma in patients with HCV-related cirrhosis. Am J Gastroenterol 103:1966–1972.

Tamori A, Nishiguchi S, Kubo S, Koh N, Moriyama Y, Fujimoto S, Takeda T, Shiomi S, Hirohashi K, Kinoshita H, Otani S, Kuroki T. 1999. Possible contribution to hepatocarcinogenesis of X transcript of hepatitis B virus in Japanese patients with hepatitis C virus. Hepatology 29:1429–1434.

Tamori A, Nishiguchi S, Kubo S, Enomoto M, Koh N, Takeda T, Shiomi S, Hirohashi K, Kinoshita H, Otani S. 2003. Sequencing of human-viral DNA junctions in hepatocellular carcinoma from patients with HCV and occult HBV infection. J Med Virol 69:475–481.

Tamori A, Nishiguchi S, Shiomi S, Hayashi T, Kobayashi S, Habu D, Takeda T, Seki S, Hirohashi K, Tanaka H, Kubo S. 2005. Hepatitis B virus DNA integration in hepatocellular carcinoma after interferon-induced disappearance of hepatitis C virus. Am J Gastroenterol 100:1748–1753.

Tanaka H, Tsukuma H, Kasahara A, Hayashi N, Yoshihara H, Masuzawa M, Kanda T, Kashiwagi T, Inoue A, Kato M, Oshima A, Kinoshita Y, Kamada T. 2000. Effect of interferon therapy on the incidence of hepatocellular carcinoma and mortality of patients with chronic hepatitis C: A retrospective cohort study of 738 patients. Int J Cancer 87:741–749.

Tanaka K, Nagao Y, Ide T, Kumashiro R, Sata M. 2006. Antibody to hepatitis B core antigen is associated with the development of hepatocellular carcinoma in hepatitis C virus-infected persons: A 12-year prospective study. Int J Mol Med 17:827–832.

Toyoda H, Kumada T, Tokuda A, Horiguchi Y, Nakano H, Honda T, Nakano S, Hayashi K, Katano Y, Nakano I, Hayakawa T, Nishimura D, Kato K, Imada K, Imoto M, Fukuda Y, Yon-Ken HCV-HCC Follow-up Study Group. 2000. Long-term follow-up of sustained responders to interferon therapy, in patients with chronic hepatitis C. J Viral Hepat 7:414–419.

Toyoda H, Kumada T, Kaneoka Y, Murakami Y. 2008. Impact of hepatitis B virus (HBV) X gene integration in liver tissue on hepatocellular carcinoma development in serologically HBV-negative chronic hepatitis C patients. J Hepatol 48:43–50.

Tsuda N, Yuki N, Mochizuki K, Nagaoka T, Yamashiro M, Omura M, Hikiji K, Kato M. 2004. Long-term clinical, virological outcomes of chronic hepatitis C after successful interferon therapy. J Med Virol 74:406–413.

Yoshida H, Shiratori Y, Moriyama M, Arakawa Y, Ide T, Sata M, Inoue O, Yano M, Tanaka M, Fujiyama S, Nishiguchi S, Kuroki T, Imazeki F, Yokosuka O, Kinoyama S, Yamada G, Omata M. 1999. Interferon therapy reduces the risk for hepatocellular carcinoma: National surveillance program of cirrhotic and noncirrhotic patients with chronic hepatitis C in Japan. IHIT Study Group. Inhibition of Hepatocarcinogenesis by Interferon Therapy. Ann Intern Med 131:174–181.

Yotsuyanagi H, Shintani Y, Moriya K, Fujie H, Tsutsumi T, Kato T, Nishioka K, Takayama T, Makuuchi M, Iino S, Kimura S, Koike K. 2000. Virologic analysis of non-B, non-C hepatocellular carcinoma in Japan: Frequent involvement of hepatitis B virus. J Infect Dis 181:1920–1928.

Liver International ISSN 1478-3223

REVIEW ARTICLE

Hepatic sinusoidal cells in health and disease: update from the 14th International Symposium

Bård Smedsrød[1], David Le Couteur[2], Kenichi Ikejima[3], Hartmut Jaeschke[4], Norifumi Kawada[5], Makoto Naito[6], Percy Knolle[7], Laura Nagy[8], Haruki Senoo[9], Fernando Vidal-Vanaclocha[10] and Noriko Yamaguchi[9]

1 Department of Cell Biology and Histology, Institute of Medical Biology, University of Tromsø, Tromsø, Norway
2 Centre for Education and Research on Ageing, University of Sydney and Concord RG Hospital, Sydney, NSW, Australia
3 Department of Gastroenterology, Juntendo University School of Medicine, Tokyo, Japan
4 Department of Pharmacology, Toxicology & Therapeutics, University of Kansas Medical Center, Kansas City, KS, USA
5 Department of Hepatology, Graduate School of Medicine, Osaka City University, Osaka, Japan
6 Department of Cellular Function, Division of Cellular and Molecular Pathology, Niigata University Graduate School of Medical and Dental Sciences, Niigata, Japan
7 Institute for Molecular Medicine and Experimental Immunology, Friedrich-Wilhelms-University Bonn, Bonn, Germany
8 Department of Nutrition, Case Western Reserve University, Cleveland, OH, USA
9 Department of Cell Biology and Histology, Akita University School of Medicine, Akita, Japan
10 Department of Cellular Biology and Histology, Basque Country University School of Medicine, Bizkaia, Spain

Keywords
hepatic stellate cell – Kupffer cell – liver – liver sinusoidal endothelial cell – sinusoid

Correspondence
Prof. Bård Smedsrød, Department of Cell Biology and Histology, Institute of Medical Biology, University of Tromsø, NO-9037 Tromsø, Norway
Tel: +47 7764 4687/+47 9959 9463
Fax: +47 7764 5400
e-mail: bard.smedsrod@fagmed.uit.no

Received 6 December 2008
Accepted 25 December 2008

DOI:10.1111/j.1478-3231.2009.01979.x

Abstract

This review aims to give an update of the field of the hepatic sinusoid, supported by references to presentations given at the 14th International Symposium on Cells of the Hepatic Sinusoid (ISCHS2008), which was held in Tromsø, Norway, August 31–September 4, 2008. The subtitle of the symposium, 'Integrating basic and clinical hepatology', signified the inclusion of both basal and applied clinical results of importance in the field of liver sinusoidal physiology and pathophysiology. Of nearly 50 oral presentations, nine were invited tutorial lectures. The authors of the review have avoided writing a 'flat summary' of the presentations given at ISCHS2008, and instead focused on important novel information. The tutorial presentations have served as a particularly important basis in the preparation of this update. In this review, we have also included references to recent literature that may not have been covered by the ISCHS2008 programme. The sections of this review reflect the scientific programme of the symposium (http://www.ub.uit.no/munin/bitstream/10037/1654/1/book.pdf):

1. Liver sinusoidal endothelial cells.
2. Kupffer cells.
3. Hepatic stellate cells.
4. Immunology.
5. Tumor/metastasis.

Symposium abstracts are refered to by a number preceded by the letter A.

Liver sinusoidal endothelial cells

Fenestrations

In his key note lecture (A1), Eddie Wisse underlined the fact that electron microscopy is still the only method of observing fenestrations in the liver sinusoidal endothelial cells (LSEC) and that sinusoidal cells of different mammalian species are amazingly similar in fine structure. He further provided information that pore size varies among species and strains and between periportal and perivenous areas of the sinusoid. After isolation, the porosity of LSECs decreases from approximately 10% at 6 h to 1% at 48 h (1) (A9). Porosity is influenced by the isolation techniques (2), the culture conditions and the presence of vascular endothelial growth factors (VEGFs) (3). Potential LSEC lines such as SKHep1 (4) might overcome some of these issues. Fenestrations are supported by actin cytoskeletal filaments, and disruption of the cytoskeleton is associated with a dramatic increase in porosity. Cellular signals involved in the regulation of actin, such as cortactin and transforming growth factor (TGF)-β1 (A15), and the Rho-like GTPases (5) influence porosity. VEGF produced by hepatocytes is probably the key cytokine involved in the regulation of LSEC fenestration mediated by actions on VEGF-R2 expressed on LSEC (6). The role of fenestrations in the bi-directional transfer of substrates between hepatocytes and sinusoidal blood is now well established (7) (A1, 13). Defenestration impairs the hepatic disposition of lipoproteins, albumin-bound drugs and other particulate substrates (7, 8) (A11, A13) and potentially impacts on T-cell interactions with hepatocytes (9). In studies using adenoviral delivery of transgene DNA, uptake of the transgene in hepatocytes correlated strongly with the LSEC pore size. The size of the adenovirus particle is 93 nm, with protruding fibres of 30 nm. Thus, the use of adenoviral-mediated gene therapy in humans may be difficult owing to the small LSEC pore size (103–107 nm) (10).

Scavenger function

Endocytic rate and capacity of LSECs are probably the highest known of any cell type in the human body. Peter McCourt presented an update on endocytosis receptors in these cells (A2). The cells carry three major types of endocytosis receptors to keep the blood clean.

The liver sinusoidal endothelial cell mannose receptor

It is known that mannose receptor (MR) clearance of several blood-borne soluble macromolecules carrying mannose in the ultimate position is carried out mainly in the LSECs, but not in the Kupffer cells (KCs) (11). Studies including MR-deficient knockout (KO) mice showed that the clearance of denatured collagen is MR mediated (12). Using the same KO mice showed that LSEC MR mediates the import of blood-borne lysosomal enzymes for re-use in the endo/lysosomal apparatus (13).

The liver sinusoidal endothelial cell scavenger receptor

Previous studies established that blood-borne negatively charged soluble macromolecular scavenger receptor (SR) ligands are cleared mainly by endocytosis in LSECs (14, 15). Hyaluronan and chondroitin sulphate, which are negatively charged connective tissue polysaccharides believed to be cleared by a highly specific hyaluronan receptor, are taken up by the same SRs that take up aminoterminal propeptides of type I and III procollagen (16). Studies employing KO mice lacking SR-A showed that the LSEC SR is distinct from SR-A (17). Recent evidence indicates that the major LSEC SR is represented by the two closely related receptors, stabilin-1 and -2 (18).

The liver sinusoidal endothelial cell Fc-γ receptor IIb2 (IIb2)

Of the known Fc-γ receptors, only IIb2 is able to mediate endocytosis of immune complexes (ICs) and only IIb2 is expressed in LSECs. Clark Anderson noted that the presence of this receptor in LSECs has, astonishingly, been ignored by immunologists (A4). Trond Berg (A5) reported that ICs endocytosed via IIb2 are degraded at a lower rate than antigens endocytosed via LSEC SR (19). Moreover, the ICs are associated with lipid rafts after cross-linking before internalization via clathrin-coated pits, and a large proportion of the internalized ICs is recycled back to the plasma membrane. Both these events delay receptor–ligand transport to later endocytic compartments. Cross-linking of LSEC IIb2 does not lead to tyrosine phosphorylation. It was suggested that the LSEC IIb2, similar to its role in dendritic cells, is able to present antigens to B-cells (A4). IIb2 in LSECs and placenta endothelium may share a similar role in local vascular immunity (20).

Comparative aspects of scavenger function

Liver sinusoidal endothelial cells represent the mammalian counterpart of vertebrate scavenger endothelial cells (SEC) (21). Using highly efficient clathrin-mediated endocytosis, these cells clear an array of colloids and soluble macromolecules from the circulation, whereas macrophages use phagocytosis to remove particles of size > 200 nm. Martin–Armas (A7) presented a study on SR-mediated endocytosis of immune-stimulating bacterial oligonucleotides, CpG (22) in Atlantic cod SEC. Preincubation of cultured cod SECs with CpG or poly I:C selectively downregulated SR-mediated endocytosis, but only marginally affected MR-mediated endocytosis. In his tutorial presentation (A6), Clive Crossley gave an update of the invertebrate scavenger cell system, the nephrocyte, which is functionally strikingly similar to the vertebrate SEC system. He focused on insect nephrocytes that display an extensively well-developed clathrin-mediated endocytosis (23). These cells endocytose ligands that are also avidly endocytosed by the mammalian LSEC SR. At present, no information is available on the structure of these receptors. Nephrocytes produce large amounts of lactate, just as the mammalian LSEC and fish SEC do. It is assumed that this lactate is used as a high-energy fuel by neighbouring energy-demanding cells.

Molecular biology

Sergij Goerdt, in his tutorial (A3), looked for LSEC-specific features in his own work and in the literature, and found that (a) stabilin-2 is lost from non-sinusoidal hepatic endothelium late in hepatic vascular differentiation (24); (b) activation of the G-protein-coupled bile acid receptor (Gpbar1/TGR5) by bile salts leads to overexpression/activation of eNOS and enhanced NO production mediating sinusoidal relaxation and hepatic stellate cell (HSC) quiescence. In contrast, endothelin (ET)-1 induces LSEC constriction and defenestration (25–28); (c) insulin is an important LSEC growth factor cross-activating the VEGF pathway (29). Moreover, endocytosis/intracellular trafficking was recently shown to be distinct in LSECs compared with other cells (30). The LSEC-specific features are as follows: (a) a remarkable net-like distribution of clathrin heavy chain, fully associated with microtubules, but not with actin; (b) clathrin-coated vesicles only partially colocalized with early endosome antigen 1 and adaptor protein 2; (c) Wnt2, an autocrine growth and differentiation factor specific for LSECs that synergizes with the VEGF signalling pathway to exert its effects (31). As a strategy to study the specialized differentiation parameters of LSECs, highly purified LSECs and lung microvascular endothelial cells (LMECs) were compared with respect to gene expression. It was found that 319 genes are overexpressed (> 4-fold) in LSECs. Interestingly, the expression of stabilin-1 and -2 were about 25 and 1000 times higher in LSECs, whereas the von Willebrand factor was 100 times higher in LMECs.

Ageing

Old age is associated with substantial thickening and defenestration of the LSEC, sporadic deposition of collagen and basal lamina in the extracellular space of Disse and increased numbers of fat-engorged, non-activated HSCs (32, 33) (A10–13). Defenestration is also apparent in isolated LSECs (A10). There is perisinusoidal upregulation of the von Willebrand factor, VEGFR-2, collagen I and IV and intercellular adhesion molecule (ICAM)-1, and reduced expression of caveolin-1 and F-actin (32). There is a 35% reduction in sinusoidal perfusion and five-fold increase in leucocyte adhesion (33) (A12). Unlike most liver diseases, there is no change in the expression of α-smooth muscle actin (α-SMA), desmin or VEGF, reduced expression of caveolin-1 and HSCs are not activated (32) (A11). These age-related changes have been termed pseudocapillarization. Pseudocapillarization is reversed by caloric restriction and resveratrol (A48). Defenestration leads to impaired transfer of lipoproteins and provides a novel mechanism and therapeutic